AIRCRAFT DIFFERENTIAL

MANEUVERING STUDIES
conducted for

NASA AMES RESEARCH CENTER
under contract NAS2-8738
during the period
February 1975
through
January 1976

Report 75-27
Calculating of Differential – Turning Barrier Surfaces

Report 75-26
A User's Guide to the Aircraft Energy – Turn
and Tandem – Motion Computer Programs

Report 75-7
A User's Guide to the Aircraft Energy – Turn
Hodograph Program
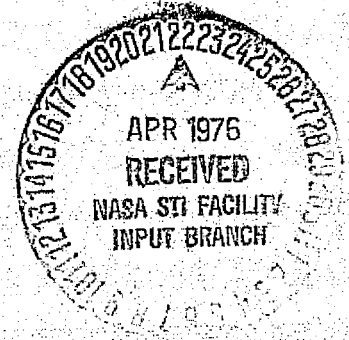
ANALYTICAL MECHANICS ASSOCIATES, INC.
50 JERICHO TURNPIKE
JERICHO, N. Y. 11753

STUDIES OF AIRCRAFT DIFFERENTIAL MANEUVERING

Henry J. Kelley and Leon Lefton

February 1976

Distribution of this report is provided in the interests of
information exchange. Responsibility for the contents
resides in the author or organization that prepared it.

FOREWORD

This report combines material generated under Contract NAS 2-8738, Aircraft Differential Maneuvering, during the period February 1975 through January 1976. It consists of updated versions of three reports issued during the period, listed as follows. The technical monitors were Dr. Mark Ardema and Mr. Michael Tauber, both of NASA-Ames Aeronautical Systems Division.

AMA Report No. 75-27, CALCULATION OF DIFFERENTIAL-TURNING BARRIER SURFACES

AMA Report No. 75-26, A USER'S GUIDE TO THE AIRCRAFT ENERGY-TURN AND TANDEM-MOTION COMPUTER PROGRAMS

AMA Report No. 75-7, A USER'S GUIDE TO THE AIRCRAFT ENERGY-TURN HODOGRAPH PROGRAM

i

CALCULATION OF

DIFFERENTIAL-TURNING BARRIER SURFACES

Henry J. Kelley
Leon Lefton

SUMMARY

The computation of composite differential-turn trajectory pairs is studied for "fast-evader" and "neutral-evader" idealizations introduced in earlier publications. Transversality and generalized corner conditions are examined and the joining of trajectory segments discussed. A criterion is given for the screening of "tandem-motion" trajectory segments. Main focus is upon the computation of barrier surfaces. Fortunately, from a computational viewpoint, the trajectory pairs defining these surfaces need not be calculated completely, the final subarc of multiple-subarc pairs not being required. Some calculations for pairs of example aircraft are presented.

INTRODUCTION

The modelling of a turning chase in air combat as a differential game with energy-modelled vehicles is described in Ref. 1 and the characteristics of families of solutions are investigated in Ref. 2. The present report, a sequel, deals with the computational solutions of families, with emphasis upon the determination of barrier surfaces, those surfaces that separate successful pursuit from successful evasion. It will be assumed, for brevity, to be read in conjunction with Refs. 1 and 2.

1

TRANSVERSALITY CONDITIONS: "FAST-EVADER" MODEL

A simplified version of the problem is of interest initially for illustrative purposes. Thus attention is directed to the "fast-evader" altitude-dynamics idealization, in which both pursuer and evader have a free choice of altitude within their respective bounds and no intervals of "tandem motion", with the pursuer driving the evader upward, appear (Ref. 2).

Consideration of a related problem with vehicle models further reduced in order (Ref. 2) suggests that fast-evader trajectory pairs have the following form. For the aircraft having the higher maximum sustainable turn rate as evader, there is simple pairing of Euler solutions terminating in the "capture set", a subset of the "target set" (both defined in Ref. 1) or on its boundary. If the sustainable-turn-rate-superior aircraft is pursuer, and if it is inferior to the evader in maximum instantaneous turn rate, some of the trajectory pairs have two subarcs. The initial subarc almost attains turn-angle closure with loft-ceiling-matched energies; the second comprises a high-turn-rate pair of trajectories joined to the first at a corner and terminates in the capture set or on its boundary.

If the capture set lies entirely above the loft-ceiling-match curve in energy space (pursuer specific energy chosen as the ordinate), capture necessarily takes place with the loft-ceiling inequality met with a margin, and both energy multiplier variables vanish at the final point by transversality. Such a situation arises in the case just mentioned exhibiting evader superiority in maximum instantaneous turn rate at matched loft-ceilings, as in Fig. 7 of Ref. 1, which applies for aircraft B pursuing A.

If the loft-ceiling-match curve forms part of the boundary of the capture set, as in Fig. 6 of Ref. 1 (A pursuing B), the energy multiplier final values for capture along the loft-ceiling-match portion will be related by transversality. With h_{L_1} and h_{L_2} the loft-ceilings for evader and pursuer, respectively, the inequality

$$h_{L_{2_f}} - h_{L_{1_f}} \geq 0 \tag{1}$$

and the equation $\Delta \chi_f = 0$, together defining capture, may be treated formally by adjoining their left members to the criterion function, final time t_f, to form the augmented function:

$$P = t_f + \Lambda_\chi \Delta \chi_f + \Lambda_{h_L} (h_{L_{2_f}} - h_{L_{1_f}}) \tag{2}$$

The usual transversality analysis leads to

$$H_f = -1 \tag{3}$$

$$\lambda_{\chi_f} = \Lambda_\chi \tag{4}$$

$$\lambda_{E_{1_f}} = -\Lambda_{h_L} \frac{dh_{L_{1_f}}}{dE_1} \tag{5}$$

$$\lambda_{E_{2_f}} = \Lambda_{h_L} \frac{dh_{L_{2_f}}}{dE_2} \tag{6}$$

Imposing these conditions at a selected terminal capture point on the loft-ceiling-match curve in energy space defines a one-parameter family of trajectory pairs, i.e., one of the two parameters Λ_χ and Λ_{h_L} is defined by (3), while the other can be regarded as the parameter of the family.

The limiting trajectory pairs corresponding to near-miss or grazing trajectories are of special interest and correspond to $H = 0$. Such pairs are not proper members of the family but define the barrier surface separating successful evasion and successful pursuit. The special values of the ratio $\Lambda_{\chi}/\Lambda_{h_L}$ that make H vanish may be determined iteratively. There may be one, two, or more of such values, or none. Some insight into this is provided by the relationship between the dual hodograph figures introduced in Ref. 1. Such a figure is drawn for loft-ceiling-matched energies using $\dot{\chi}$ for the ordinate and $(dh_L/dE)\dot{E}$ for the abscissa. The number of intersections of the two hodograph figures in the upper quadrants equals the number of vanishings of H. If one figure lies entirely within the other, there are none; this means one aircraft is locally superior and that there are no grazing trajectories through the point. An intersection in the upper quadrants implies $H = 0$ by the existence of a common tangent to the figures; a perpendicular to this through the origin defines the direction of the corresponding multiplier vector. The term "tangent" is employed loosely here to include contact at a corner of the figure.

COMPOSITE "FAST-EVADER" TRAJECTORIES

If the pursuer does not have any kind of low-energy superiority, the trajectory pairs are unbroken (except for what might be called "ordinary" corners, those satisfying the Erdmann condition) and can be found by integration of Euler solutions backwards in time using final multiplier values determined from eqs. (3)-(6); trajectories terminating at various points of the capture set's boundary computed in this way determine the barrier surface.

What might be called generalized corners, i.e., corners with multiplier jumps, appear when the pursuer is superior in maximum sustainable turn rate and at the same time inferior in maximum instantaneous turn rate along the matched-loft-ceiling curve in energy space. When the opposing aircraft have this relationship, the pursuer, even having attained near angular closure with sufficient energy, is unable to effect capture immediately but only manages to force the evader into a high-turn-rate maneuver and to steer the chase toward lower energies where capture may take place. It can be argued that sustainable-turn-rate-superiority of the pursuer along the matched-loft-ceiling curve to the lowest energies permitting flight makes closure with matched-loft-ceiling energy tantamount to subsequent capture. The appearance of at least some such two-subarc trajectories is insured with less overwhelming superiority, i.e., superiority of pursuer in maximum sustainable turn rate with energies of both craft unrestricted; in this case, a segment of the matched-loft-ceiling curve will be the locus of generalized corner junctions. The upper end of this segment is defined by the limit of the pursuer's sustainable-turn-rate superiority. The lower end will be on or below the lower edge of the band of pursuer energies defined by pursuer sustainable turn rate superiority over the evader's highest sustainable turn rate determined with his energy unrestricted. The arguments needed to establish that closure with matched-loft-ceiling energy along this segment insures subsequent capture are elementary and similar to those employed for the sufficient condition of Ref. 1.

Attention is now directed to the generalized corner junction of extremals appearing in this case where the pursuer has superiority at low energy but lacks a margin of maximum instantaneous turn-rate to turn closure immediately into capture at high energy.

Consider a family of Euler solutions through an initial point having $\Delta\chi > 0$ and pursuer energy high enough that some of the family members intersect $\Delta\chi = 0$ above the lost-ceiling-match curve. Call $T(E_1, E_2)$ the time-to-capture measured from arrival at $\Delta\chi = 0$, and Δt (not necessarily small) the time elapsed during the motion along the first subarc. Then an augmented performance index may be set up as

$$P = T(\bar{E}_1, \bar{E}_2) + \Delta t + \nu(\bar{h}_{L_2} - \bar{h}_{L_1}) + \bar{\Lambda}_\chi \, \bar{\Delta}\chi \tag{7}$$

where the superscribed bars denote values at arrival at the surface $\Delta\chi = 0$. If the inequality

$$\bar{h}_{L_2} - \bar{h}_{L_1} \geq 0 \tag{8}$$

is met with a margin, then $\mu = 0$. The equality will obtain in many cases, however, since the pursuer will generally tend to sacrifice energy margin for turn-rate in effecting closure.

A transversality analysis carried out with the inequality (8) and $\Delta\chi = 0$ regarded as an intermediate target set leads to the system:

$$\bar{H} = -1 \tag{9}$$

$$\bar{\lambda}_\chi = \bar{\Lambda}_\chi \tag{10}$$

$$\bar{\lambda}_{E_1} = \frac{\partial T}{\partial \bar{E}_1} - \nu \frac{dh_{L_1}}{dE_1} \tag{11}$$

$$\bar{\lambda}_{E_2} = \frac{\partial T}{\partial \bar{E}_2} + \nu \frac{dh_{L_2}}{dE_2} \tag{12}$$

For extremal subarcs entering the surface $\Delta\chi = 0$ with strict inequality ($>$) in (8), $\nu = 0$ and the conditions (9)-(12) determine all of the multipliers. For $\nu \neq 0$, there is a one-parameter family whose limiting members occur for ν unbounded; these are not proper members, as $\overline{H} = 0$. The ratio of multipliers

$$\overline{\lambda}_{E_1} \Big/ \overline{\lambda}_{E_2} = \frac{dh_{L_1}}{dE_1} \Big/ \frac{dh_{L_2}}{dE_2} \tag{13}$$

is well defined in the limit. These multipliers and λ_χ are defined only within a multiplicative constant for these grazing trajectories. (Note that this corresponds to the classical definition of abnormality in variational problems: nonuniqueness of the multipliers.)

The generalized corner condition of Bernhard (Ref. 3) furnishes a guide to which components of the multiplier vector jump and which do not, viz. the jump is normal to the singular surface. For $\nu = 0$, this surface is the portion of the plane $\Delta\chi = 0$ above the matched-loft-ceiling curve, and only the multiplier λ_χ jumps. For $\nu \neq 0$, it is the boundary defined by the equality sign in (8), and the energy multipliers jump to their values $\partial T/\partial E_1$ and $\partial T/\partial E_2$ from the values (11) and (12); there is no jump in the component of the energy-multiplier vector along the loft-ceiling-match curve's tangent.

Constructing nongrazing trajectory pairs that have two subarcs and terminate in capture from the first-order necessary conditions is fairly laborious. First, "open-loop" trajectory pairs connecting the capture set and the intermediate target set defined by (8) and $\Delta\chi = 0$ are obtained. These are the second subarcs of composites and their energy multipliers provide the partials $\partial T/\partial E_1$ and $\partial T/\partial E_2$ needed in (11) and (12). The system (9)-(12) then provides multiplier end conditions for backward integration of Euler solutions which are the appropriately matched first subarcs.

A stroke of good fortune is that grazing trajectory pairs, of main interest because they define the barrier, are relatively easy to calculate. This limiting case has the first-subarc terminal values independent of the second-subarc solution; the partials $\partial T/\partial E_1$ and $\partial T/\partial E_2$ do not appear in (13), which greatly simplifies the calculation of the barrier surfaces. A similar situation occurs with the neutral-evader model, to be taken up next.

"NEUTRAL-EVADER" MODEL

Adoption of the more realistic "neutral-evader" model leads to families of solutions having a more complex structure, as discussed in Ref. 2. Under circumstances somewhat similar to those in which two-subarc solutions arise with the simpler model, solutions having a third, middle, subarc of so-called "tandem motion" appear. The tandem motion may itself be complex, including the singular arcs discussed in Ref. 2. The discussion of this section will ignore the possible appearance of singular subarcs, whose rôle is not fully understood at present. It is worth noting, however, that all of the singular subarcs found computationally in the examples to date have been screened out by one test or another, hence the assumed non-appearance may not be unduly restrictive.

Trajectories of "tandem-loft" type, calculated by the procedure and computer program described in Ref. 4, are shown in energy space in Fig. 3 for aircraft B as pursuer and A as evader. There is one trajectory of particular interest that bifurcates, dividing the family. Those above it generally produce a loss of pursuer energy and originate at high pursuer energies. Those below the bifurcating trajectory correspond generally to increasing pursuer energy (although not monotonically), and originate at low pursuer energies. The two branches of the bifurcating trajectory form a separatrix, a boundary outside of which the tandem-loft motion does not attain loft-ceiling match.

The family of tandem/loft trajectories is determined by numerical integration using a computer program such as that described in Ref. 4. As a preliminary, loft-ceiling rates at matched-loft-ceiling altitudes may be compared at various points along the loft-ceiling-match curve in energy space, as in Fig. 5 of Ref. 2. This was carried out with the computer program of Ref. 5, which also performs a single step of integration backwards in time using a coarse integration technique

(Euler extrapolation) to assist the search for the bifurcating trajectory and the separatrix.

The region in energy space between the separatrix and the loft-ceiling-match curve plays a rôle in the neutral-evader trajectory family analogous to that of the loft-ceiling-match curve in that of the simpler fast-evader model. Trajectory pairs corresponding to pursuer closure with insufficient energy undergo transitions in this region to tandem-loft motion, which may continue until the loft-ceiling-match curve is reached; then either capture occurs or a transition to a high-turn-rate open-loop-optimal pair. The grazing trajectories for $H = 0$ join with tandem-loft arcs on the separatrix when the hodograph figures are in the proper relationship, previously described; however, the scaling factors on the energy-rate axes of these figures are different: they are the magnitudes of the energy multipliers. The ratio of these is of main importance, and, along the separatrix, this ratio for $H = 0$ is obtained as

$$\left| \frac{\lambda_{E_2}}{\lambda_{E_1}} \right| = \left| \frac{\dot{E}_1}{\dot{E}_2} \right| \tag{14}$$

This may be viewed as the determination of the normal to a two-dimensional trajectory from the components of velocity. The relationship (14) is employed like (13) in the determination of multipliers from transversality conditions generally similar to those given for the fast-evader model. The computation of barrier candidates comes down to the use of (14) for the energy-multiplier ratio together with $H = 0$ solved iteratively for the ratio of λ_X to one of the energy multipliers.

The segment of the separatrix which is the locus of generalized corners for barrier trajectory pairs is simply related to the corresponding segment of the loft-ceiling-match curve discussed previously for the fast-evader model. The relating property is that tandem-loft trajectory pairs originating on the separatrix segment

10

must remain within a region in energy space characterized by the existence of at least one dual-hodograph-figure intersection and reach the matched-loft-ceiling curve, otherwise a transition to 3-D motion and successful evasion is possible. The argument is similar to that for the sufficient condition of Ref. 1. In the example of aircraft B chasing A , the entire separatrix maps into a single point on the loft-ceiling-match curve which is within the region of pursuer-superior sustainable turn rate (shaded in Fig. 3) and hence well within the intersecting-dual-hodograph region.

It appears possible that the locus of generalized corners of barrier trajectories in energy space may sometimes be a composite including segments of the separatrix, the boundary of the intersecting-dual-hodograph region between the separatrix and the loft-ceiling-match curve, and the loft-ceiling-match curve itself. Along the intersecting-dual-hodograph boundary, the multiplier ratio analogous to (13) and (14) may be obtained from the normal to the boundary.

THE COMPUTATION OF BARRIER SURFACES

Families of trajectory pairs integrated backwards in time numerically define the barrier surfaces. All start at $\Delta\chi = 0$ and at pairs of specific energies along the types of curves in the energy space previously discussed. Multiplier values are determined as discussed in the preceding sections. The present section discusses the procedure and sequence of calculations employed with computer programs such as those of Refs. 4 and 5.

Perform first a comparison of energy rates and sustainable turn rates with energies matched over the energy range for equal loft-ceilings. The computation of the barrier surface for the sustainable-turn-rate-superior aircraft as evader proceeds entirely from the boundary of the capture region. If this lies completely above the loft-ceiling-match curve, the boundary is defined by matching of maximum instantaneous-turn-rates; if not, some portion of the loft-ceiling-match curve itself may form a portion of the boundary. The energy multiplier end values are zero for maximum-instantaneous-turn-rate match and given by (13) for loft-ceiling match. The value of λ_χ is found in the latter case from $H = 0$. The program of Ref. 4 does this by a scan followed by an iteration. If two values of λ_χ emerge from this computation, one of them may be of interest when the aircraft pursuer/evader rôles are reversed.

For the sustainable-turn-rate-superior craft as pursuer, segments of the loft-ceiling-match curve, the separatrix, and the sustainable-turn-rate boundary may form part of the locus of generalized corners of barrier trajectories. If there is a region of tandem/loft motion that leads to loft-ceiling match, the separatrix should be found, then a composite locus of generalized corners for barrier trajectories by examining the tandem-loft trajectory family relative to the sustainable-turn-rate-superiority region of the pursuer.

COMPUTATIONAL RESULTS FOR A VERSUS B

Some results are presented in Figs. 1, 2, and 4 of barrier surfaces for turning duels between aircraft A, a hypothetical Mach 3 design, and aircraft B, a version of the F-4 used for illustrative computations in Refs. 1 and 2.

Figure 1 applies for A chasing B; it is the same for both fast-evader and neutral-evader models. The upper boundary of the capture set is the instantaneous-turn-rate-match curve, while the lower is the loft-ceiling-match curve. Integrations of trajectory pairs never develop appreciable positive $\Delta\chi$ values except at high energies; even in the region most favorable to A, only small angle differences can be closed successfully.

Figure 2 is for fast-evader modelling, B chasing A. The trajectory pairs defining the barrier all pass through the lower portion of the loft-ceiling-match curve.

Figure 3 shows the region of tandem motion for B chasing A and the separatrix arising from bifurcation of a tandem/loft trajectory that divides the region. All of the tandem trajectories considered are of tandem/loft type, since all chattering singular arc segments are screened out by failure to meet one requirement or another (Ref. 2). The pursuer-sustainable-turn-rate region is shown shaded.

Figure 4 shows the barrier surface for B chasing A, neutral-evader modelling. The trajectory pairs defining the barrier pass through the separatrix, only a small upper portion of the separatrix proving barren. The difference between the barrier results for fast-evader and neutral-evader models is large in this example and implies that the tandem/loft pursuit tactic is important. It should be noted that this may be untypical because of an anomaly in the otherwise realistic data for

aircraft A : $C_{L_{max}}$ was taken as unity independent of Mach number; this is an especially optimistic figure supersonically. This leads to an energy-rate advantage for B when both craft fly at matched-loft-ceiling altitude, hence favors the lofting tactic for B as pursuer.

RESULTS FOR B VERSUS C WITH PARAMETERIZED THRUST

Shown next are some results for aircraft B (F-4) against C, a version of the F-5. B can reach substantially higher energies than C (110 K vs. 70 K); however, it is inferior to C in both maximum sustainable turn rate and maximum instantaneous turn rate at matched loft-ceilings. The mismatch in capabilities between B and C resembles somewhat the mismatch seen in the preceding example between A and B, but is not as extreme. The trajectory families are simpler in two respects: the opportunities for successful tandem-lofting pursuit are negligible (and have been omitted entirely in the computations), and the relationship between maximum instantaneous turn rates is such that high-turn-rate spirals to low energy occur only for B chasing C, i.e., C can capture at high energy. Taken together, these characteristics result in simple pairing of trajectories in all cases; there are no multiple-subarc trajectories in the families.

Figure 5 presents barrier-surface results for B pursuer and C evader. Successful pursuit occurs only for C in the low energy range and for B with a large initial energy advantage in combination with an angular position advantage.

Figure 6 shows barrier data for C chasing B. Generally, an energy advantage is needed by C to capture B before the chase reaches B's high-energy haven. Given such an advantage, C can close fairly large angular gaps and capture when the initial energies are low; however, at high initial energies, only modest closures can be effected even with large energy advantage.

A computational study of barrier behavior as B's thrust level is increased was carried out. An important guide to the behavior is provided by the sustainable-turn-rate boundaries in energy space depicted in Figure 7. Configuration B2 has 20% thrust increase over the basic value over the entire Mach number/altitude range,

B3 30%, B4 40%. The situation is similar to that of the B/A example as in Fig. 3, although simpler in respect to the absence of tandem/loft motion. As the thrust is increased from 30% to 40% over basic, B develops an overall superiority in maximum sustainable turn rate, energy choice open, and the barrier surface for B pursuing C disappears, implying eventual capture in a long-duration chase irrespective of initial conditions. Barrier surfaces in Figs. 8, 9, and 10 show the shifts in capture capability as B's thrust is increased. The results shown are only rough approximations on account of coarseness of mesh of the trajectory data.

RESULTS FOR A TRAPEZOIDAL-WING RPV CONFIGURATION

Some calculations were carried out for the high-performance RPV configuration of Ref. 6. Maximum instantaneous turn rate, maximum sustainable turn rate, and maximum loft-ceiling rate versus energy are shown for this configuration, designated D, in Fig. 11, where the corresponding characteristics of aircraft B are also shown for comparison. The superiority of D over B is overwhelming; the sufficient condition of Ref. 1 is met and eventual capture in rôle-determined D/B engagements is insured irrespective of initial conditions.

A similar comparison of hodograph data for D and A is shown in Fig. 12. D is seen to be superior in the dogfighting energy range; the superiority wanes above 100 K energy because of inlet off-design characteristics. The barrier results of Fig. 13 show A incapable of capture except at extremely low evader energy and then only with tremendous energy and angular position advantages. The barrier surface of Fig. 14 indicates high effectiveness of D pursuing A except at high energies near A's haven. Fragmentary trajectory data in the energy range 60-100 K indicate that the poorly-defined barrier surface may actually fold over into the region below the loft-ceiling-match curve (marked No Capture) for large angular separation; there is some difficulty in representing the surface graphically here, in addition to a coarseness-of-mesh problem.

CONCLUDING REMARKS

A procedure has been presented for the calculation of barrier surfaces for differential-turning duels and examples given. Three computer programs, each fairly complex, were used and a certain amount of crossplotting of intermediate data was required in the first computational example; however, considerable streamlining of the programs and computations was carried out in the process of the subsequent applications and the generation of barrier surface data can be regarded as a practical proposition for engineering applications work.

REFERENCES

1.   Kelley, H. J.; "Differential-Turning Optimality Criteria," Journal of Air-
      craft, January 1975.

2.   Kelley, H. J.; "Differential-Turning Tactics," AIAA Mechanics and Control
      of Flight Conference, Anaheim, California, August 5-8, 1974; to appear
      in Journal of Aircraft.

3.   Bernhard, P.; "Corner Conditions for Differential Games," Fifth IFAC
      Congress, Paris, France, June 12-17, 1972.

4.   Lofton, L., Krenkel, A. R. and Kelley, H. J.; "A User's Guide to the Air-
      craft Energy-Turn and Tandem Motion Computer Programs," Analytical
      Mechanics Associates, Inc. Report No. 75-26, June 1975; revised edition,
      January 1976.

5.   Lefton, L. and Kelley, H. J.; "A User's Guide to the Aircraft Energy-
      Turn Hodograph Program," Analytical Mechanics Associates, Inc. Report
      No. 75-7, March 1975; revised edition, January 1976.

6.   Nelms, W. P. and Axelson, J. A.; "Preliminary Performance Estimates
      of a Highly Maneuverable Remotely Piloted Vehicle," NASA TN D-7551,
      February 1974.

FIGURE 1

BARRIER SURFACE

Pursuer/Evader   A/B

No Capture

Initial Angular
Separation .15 rad.

100

120

E_A
Pursuer
Specific
Energy
ft. x 10^{-3}

80

60

$\triangle \chi = 0$

Capture

No Capture

40

Initial Angular
Separation 0 rad.

20

0

0   20   40   60   80   100   120

E_B

Evader Specific Energy – ft. x 10^{-3}
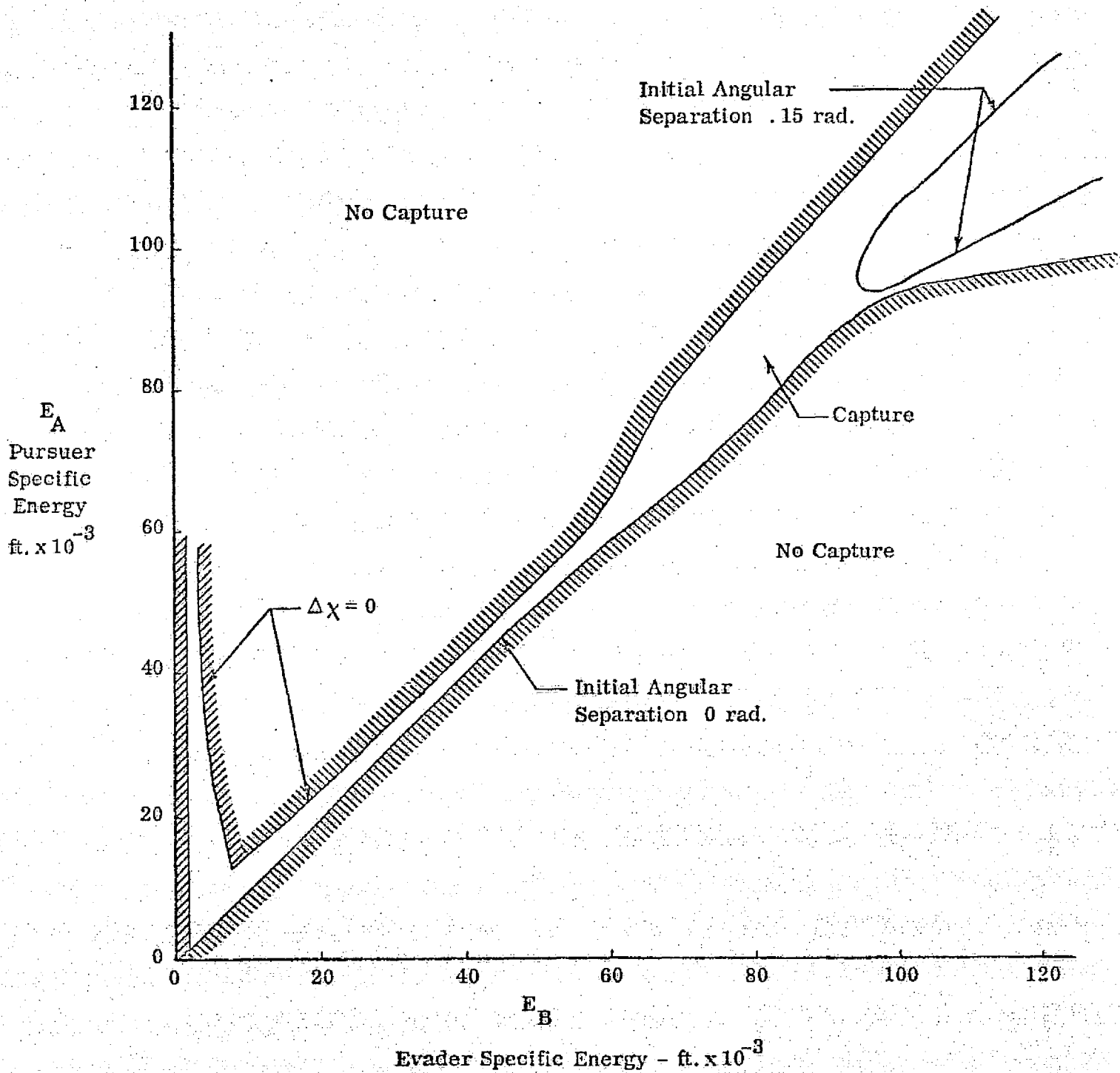
FIGURE 2

BARRIER SURFACE

'Fast-Evader' Model

Pursuer/Evader   B/A
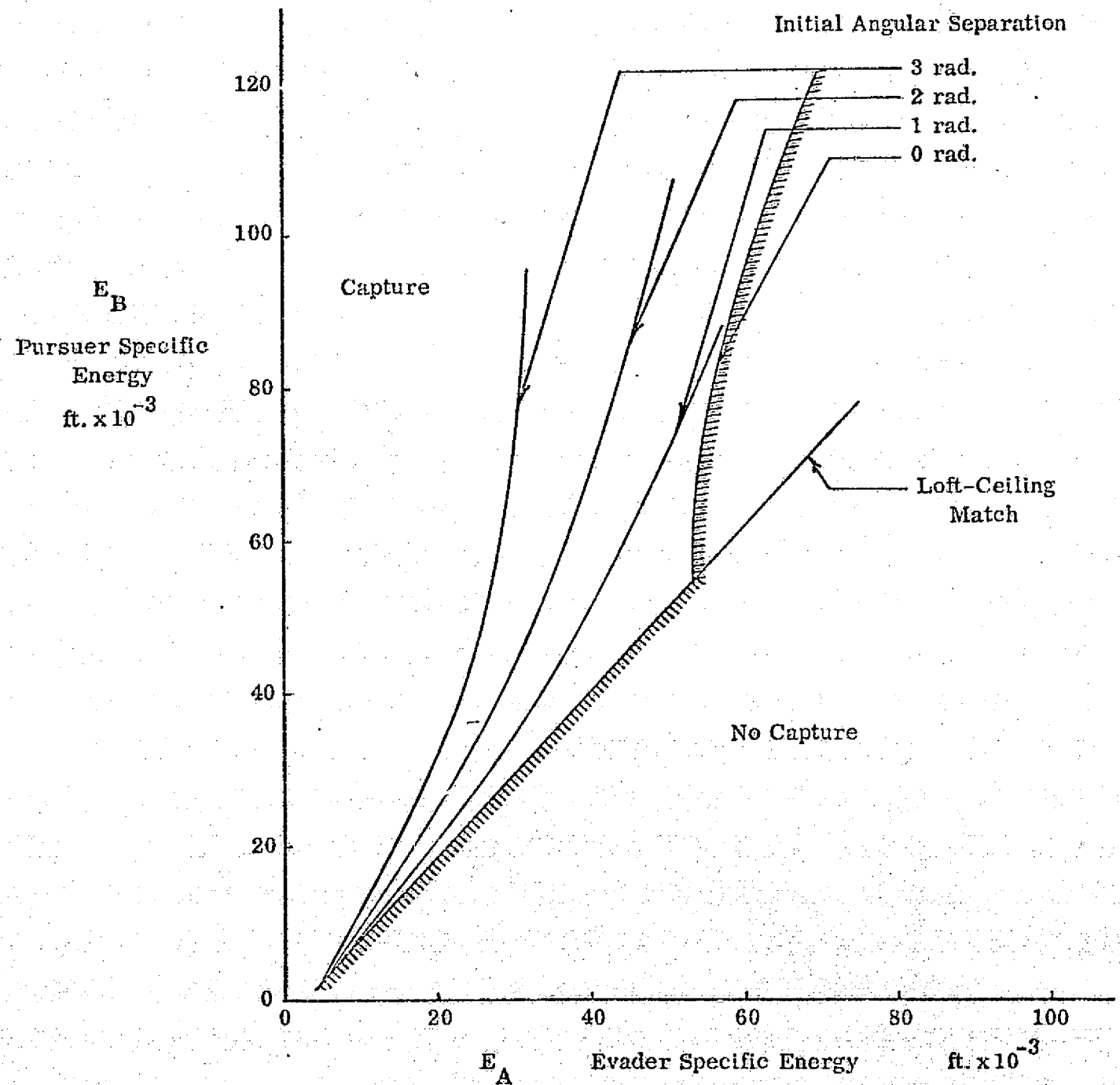
FIGURE 3
TANDEM/LOFT TRAJECTORIES
AND SEPARATRIX

Pursuer Energy E_{PB} ft x 10^{-3}

Evader Energy E_{EA} ft x 10^{-3}

Loft–Ceiling Match
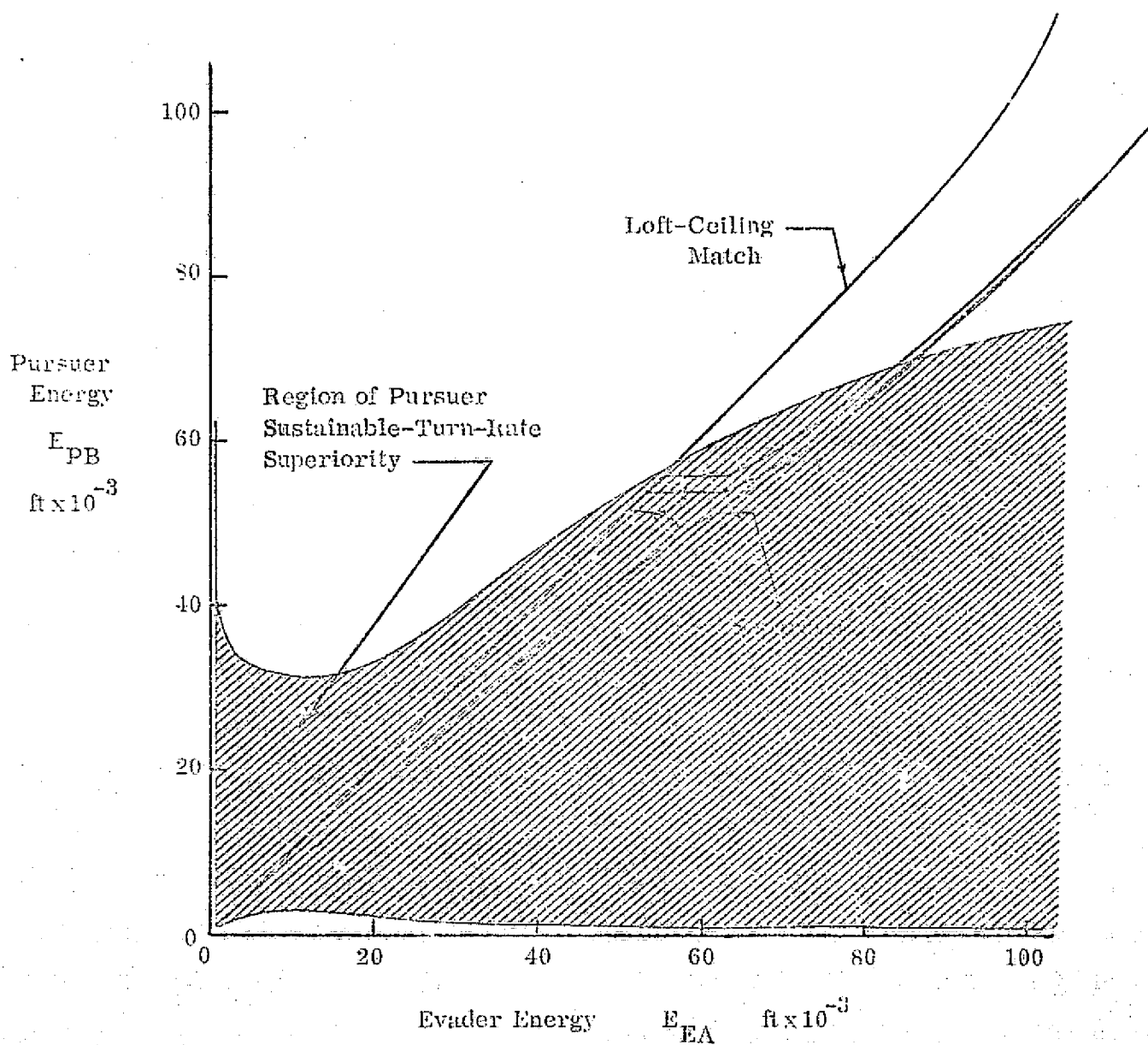
Region of Pursuer Sustainable–Turn–Rate Superiority

FIGURE 4

BARRIER SURFACE

'Neutral-Evader' Model

Pursuer/Evader   B/A
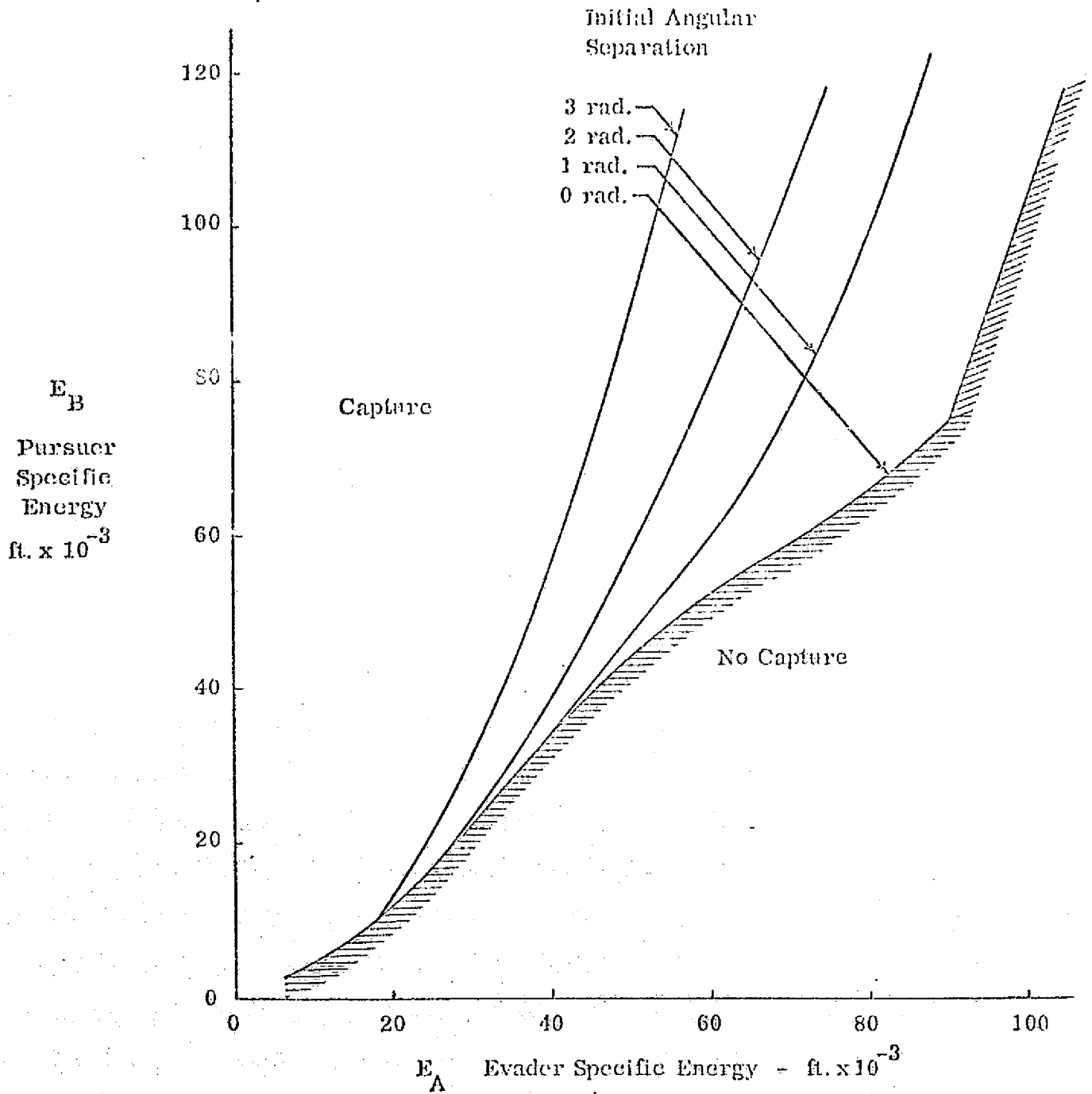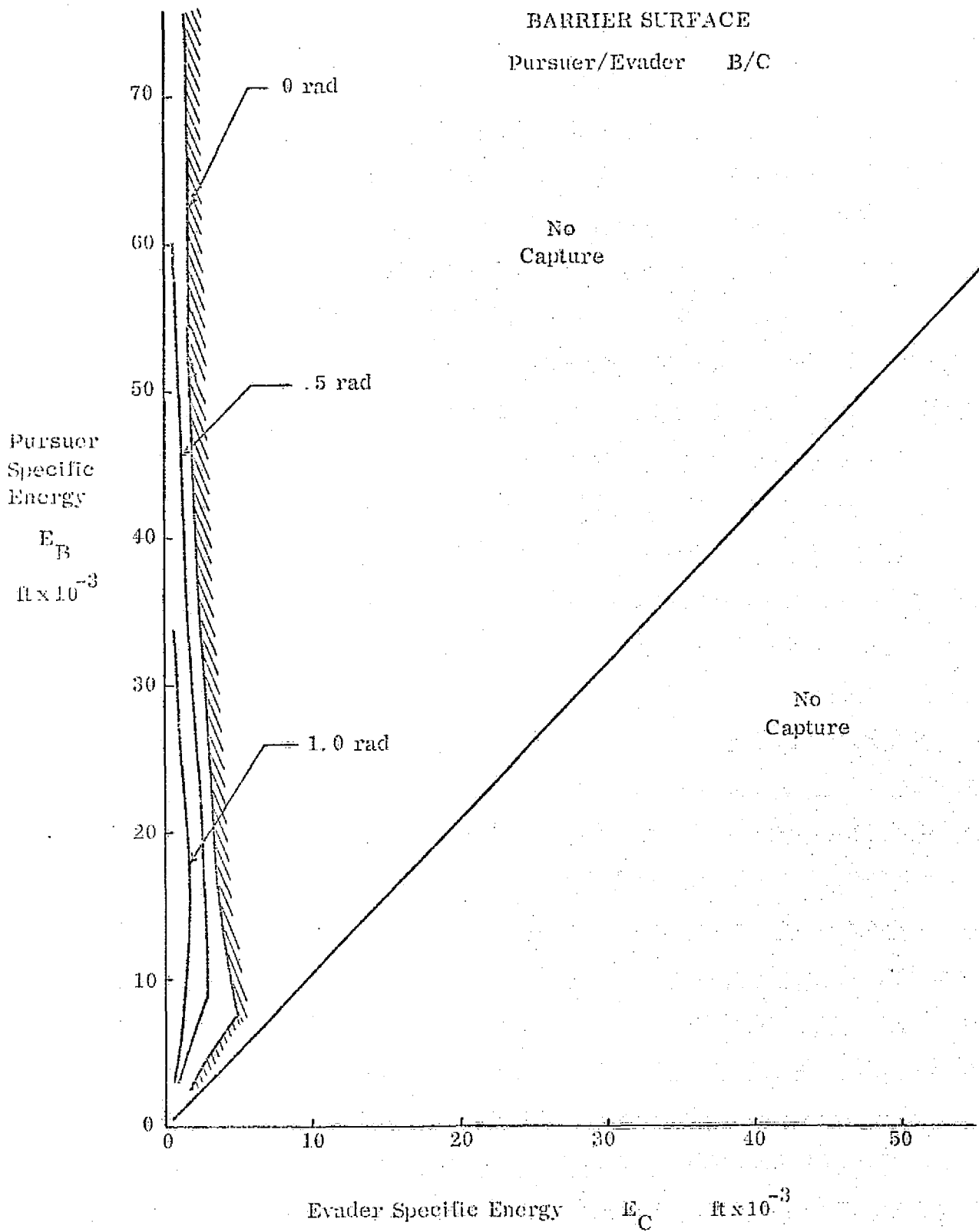
FIGURE 5

BARRIER SURFACE

Pursuer/Evader   B/C

FIGURE 6

BARRIER SURFACE

Pursuer/Evader   C/B

Pursuer Specific Energy

E_C

$ft \times 10^{-3}$

Evader Specific Energy E_B $ft \times 10^{-3}$
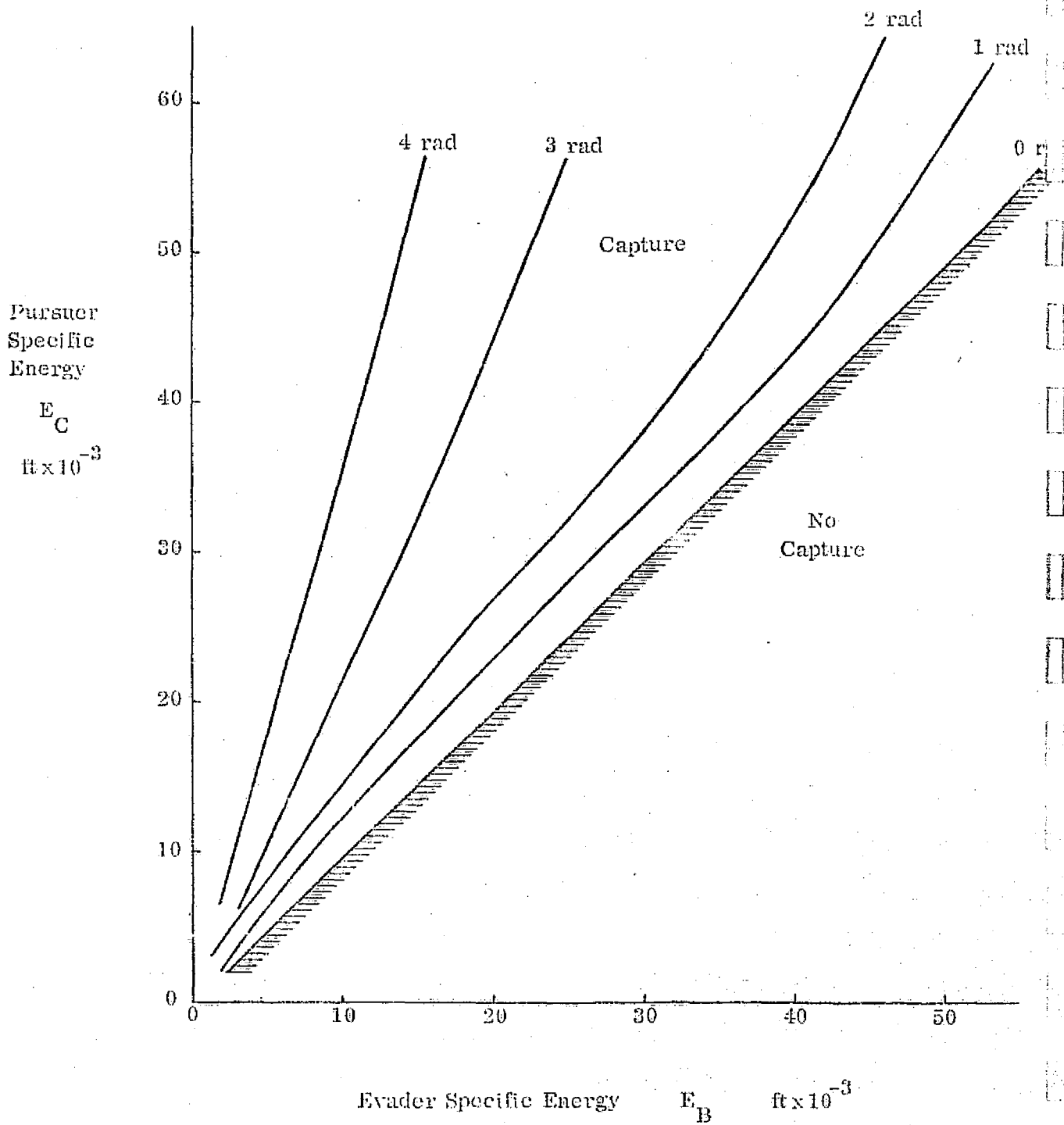
FIGURE 7

SUSTAINABLE-TURN-RATE-SUPERIORITY REGIONS

Pursuer B, B3, B4

Evader C

Pursuer
Specific
Energy

E_B

$ft \times 10^{-3}$

B Superior
B3 Superior
B4 Superior

Evader Specific Energy E_C $ft \times 10^{-3}$
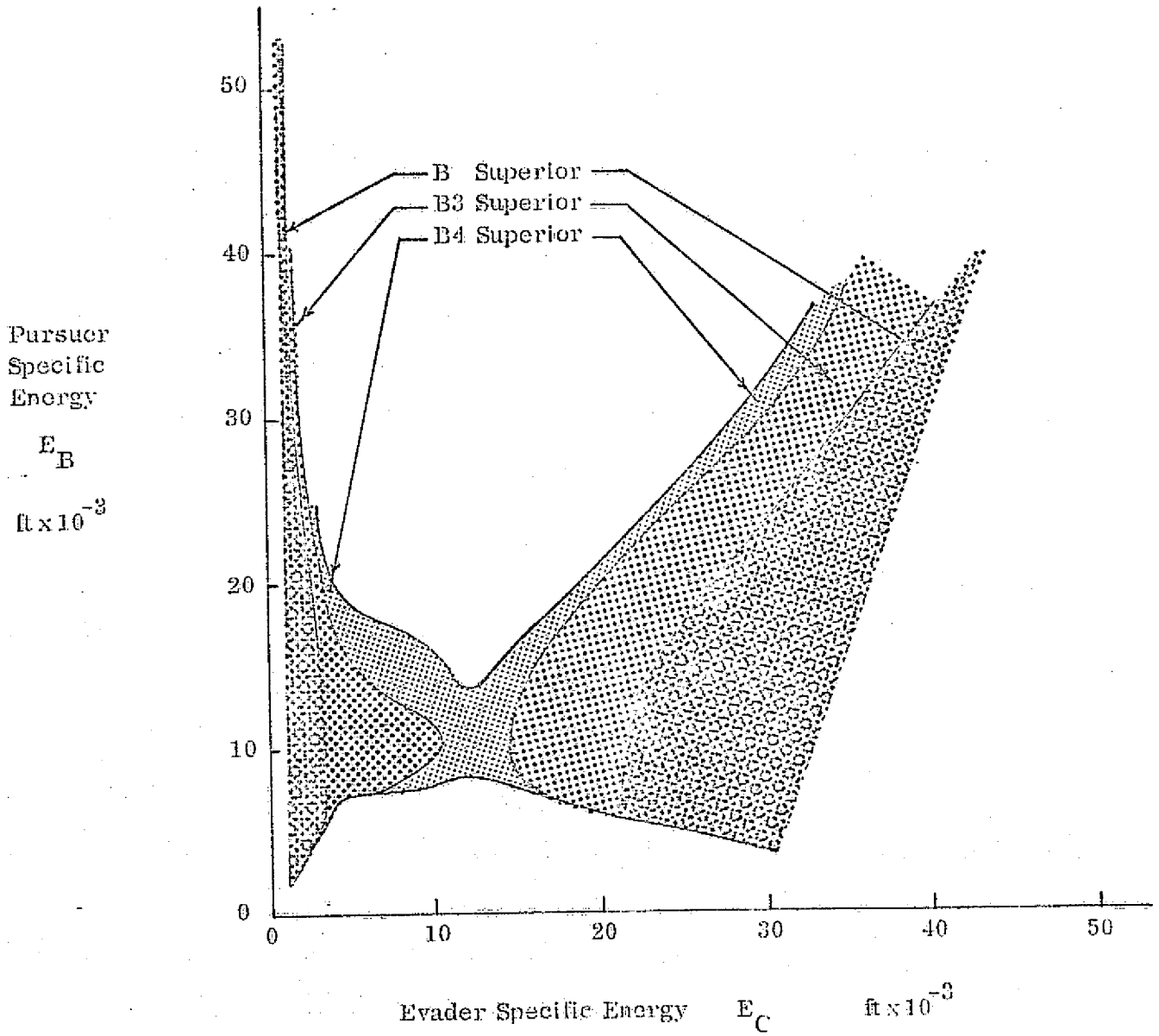
FIGURE 8

BARRIER SURFACE

Pursuer/Evader   B2/C
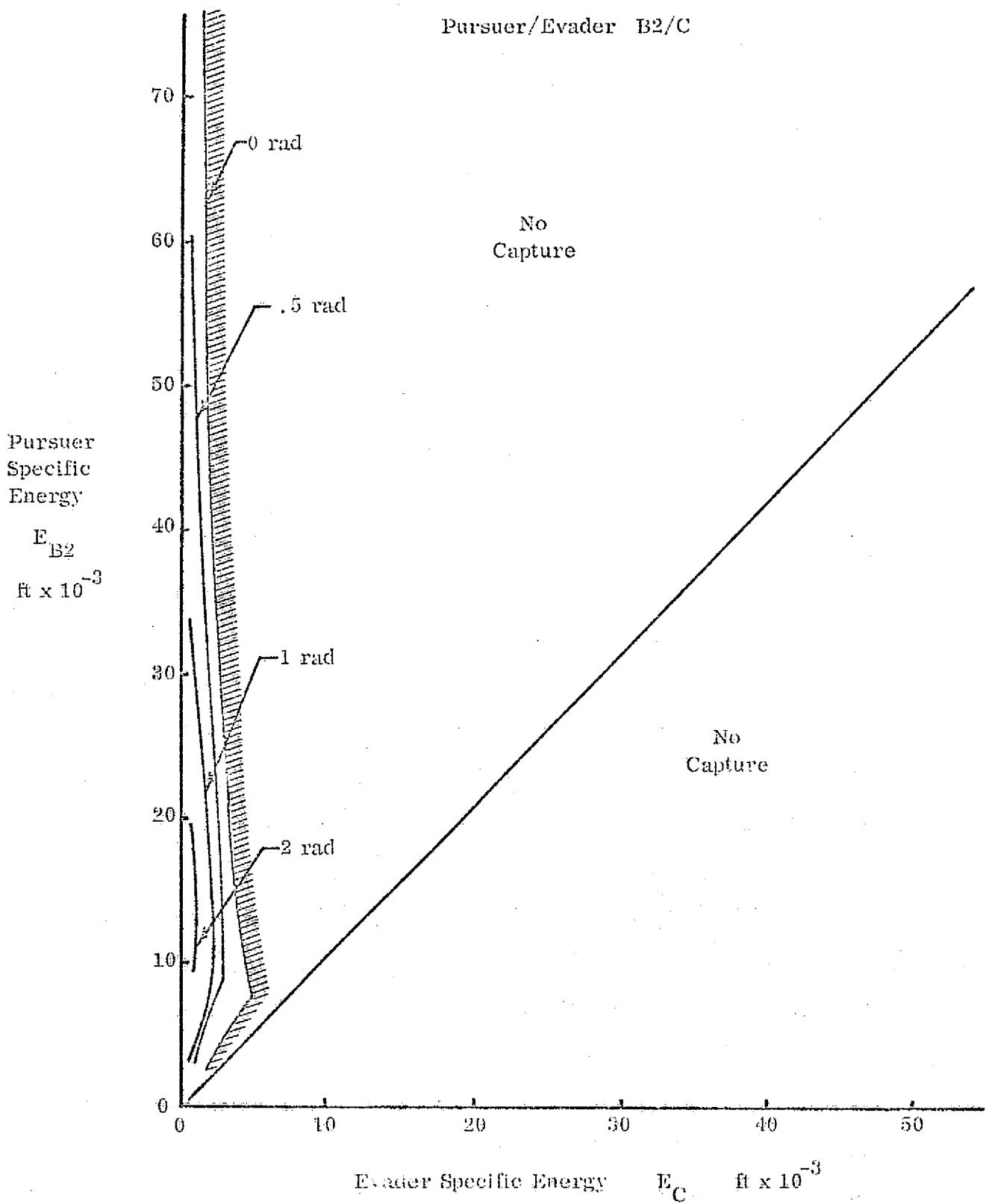
FIGURE 9

BARRIER SURFACE

Pursuer/Evader   C/B2
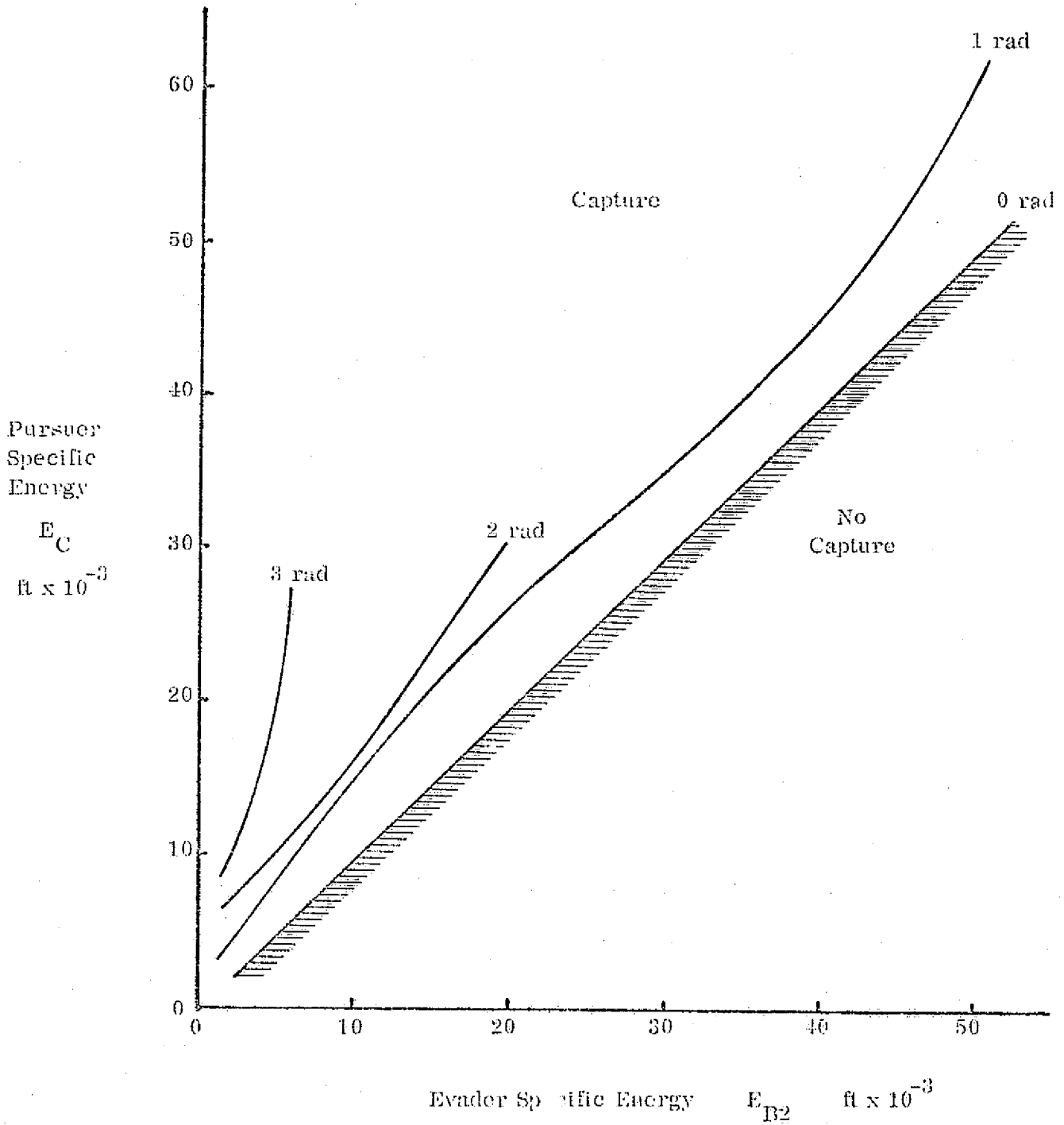
FIGURE 10

BARRIER SURFACE

Pursuer/Evader   C/B3
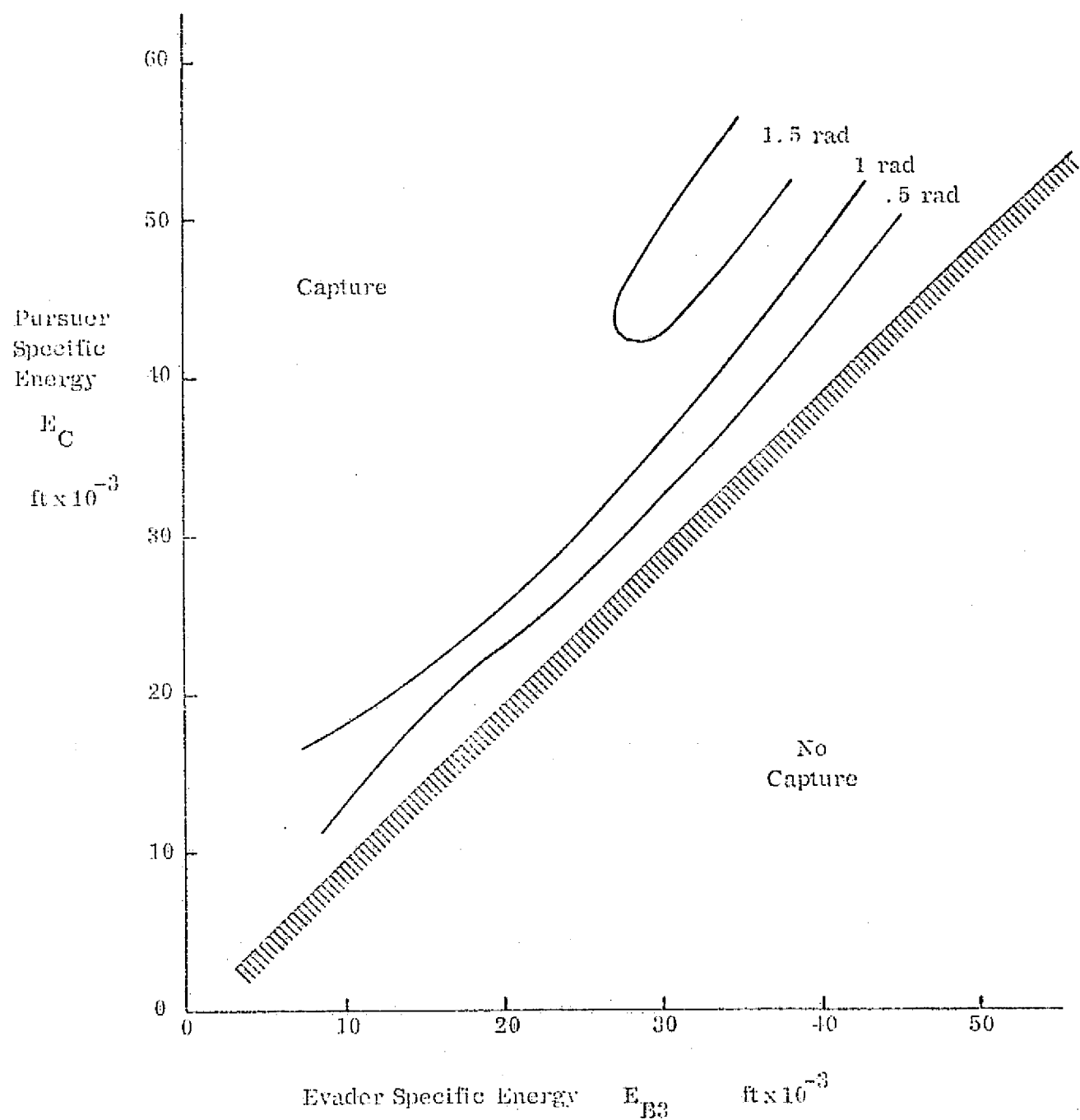
FIGURE 11

HODOGRAPH COMPARISON AT

MATCHED LOFT-CEILING ENERGIES

Configurations B & D
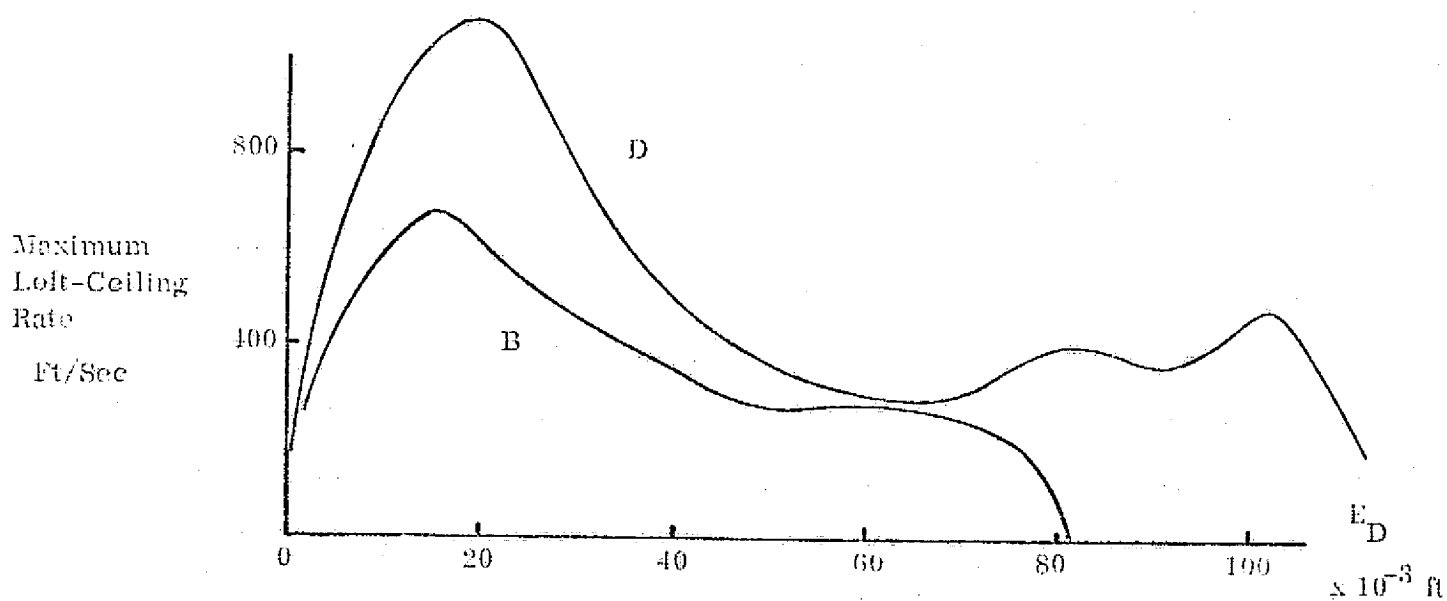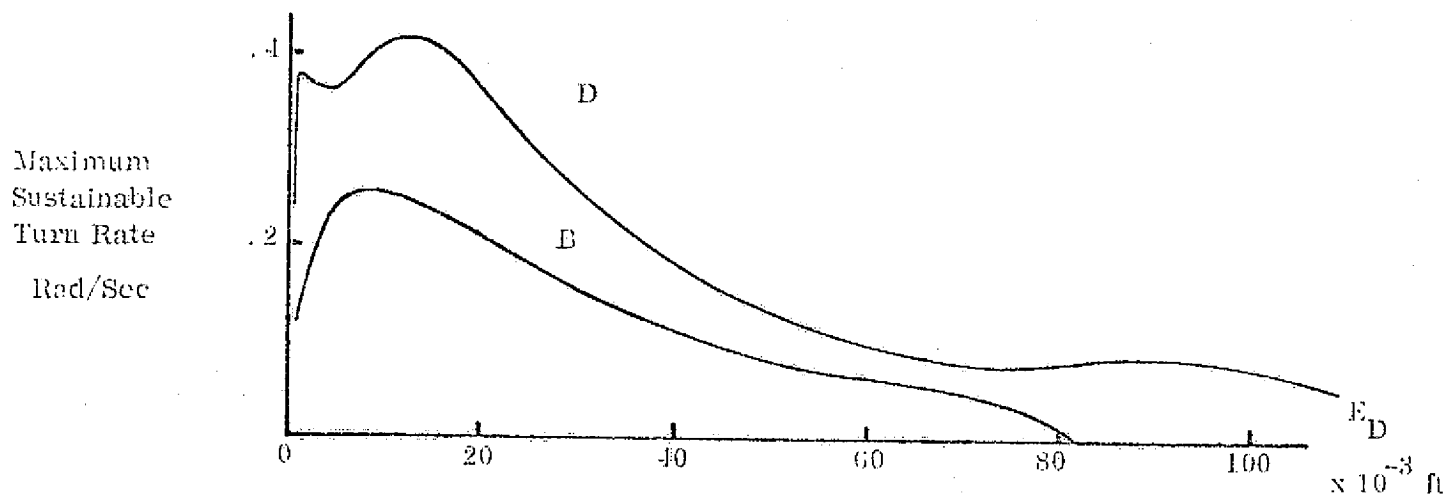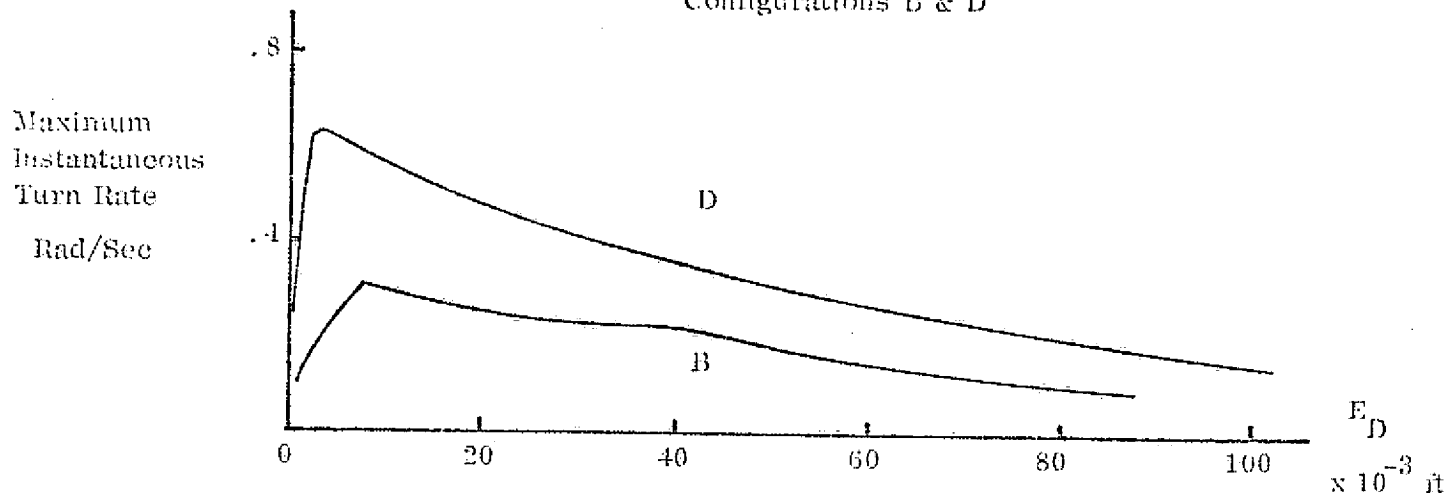
FIGURE 12

HODOGRAPH COMPARISON AT

MATCHED LOFT-CEILING ENERGIES

Configurations A & D

FIGURE 13

BARRIER SURFACE
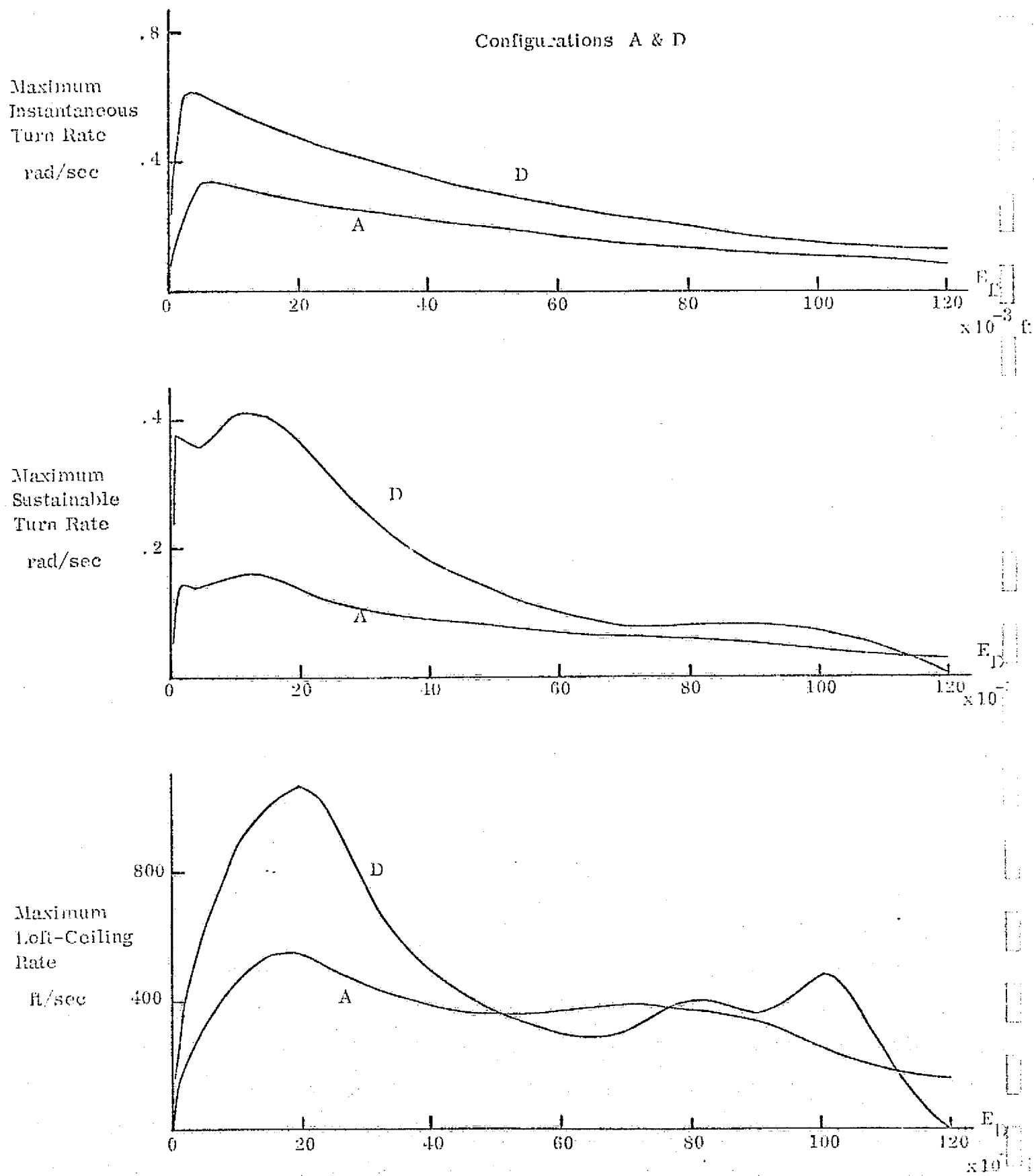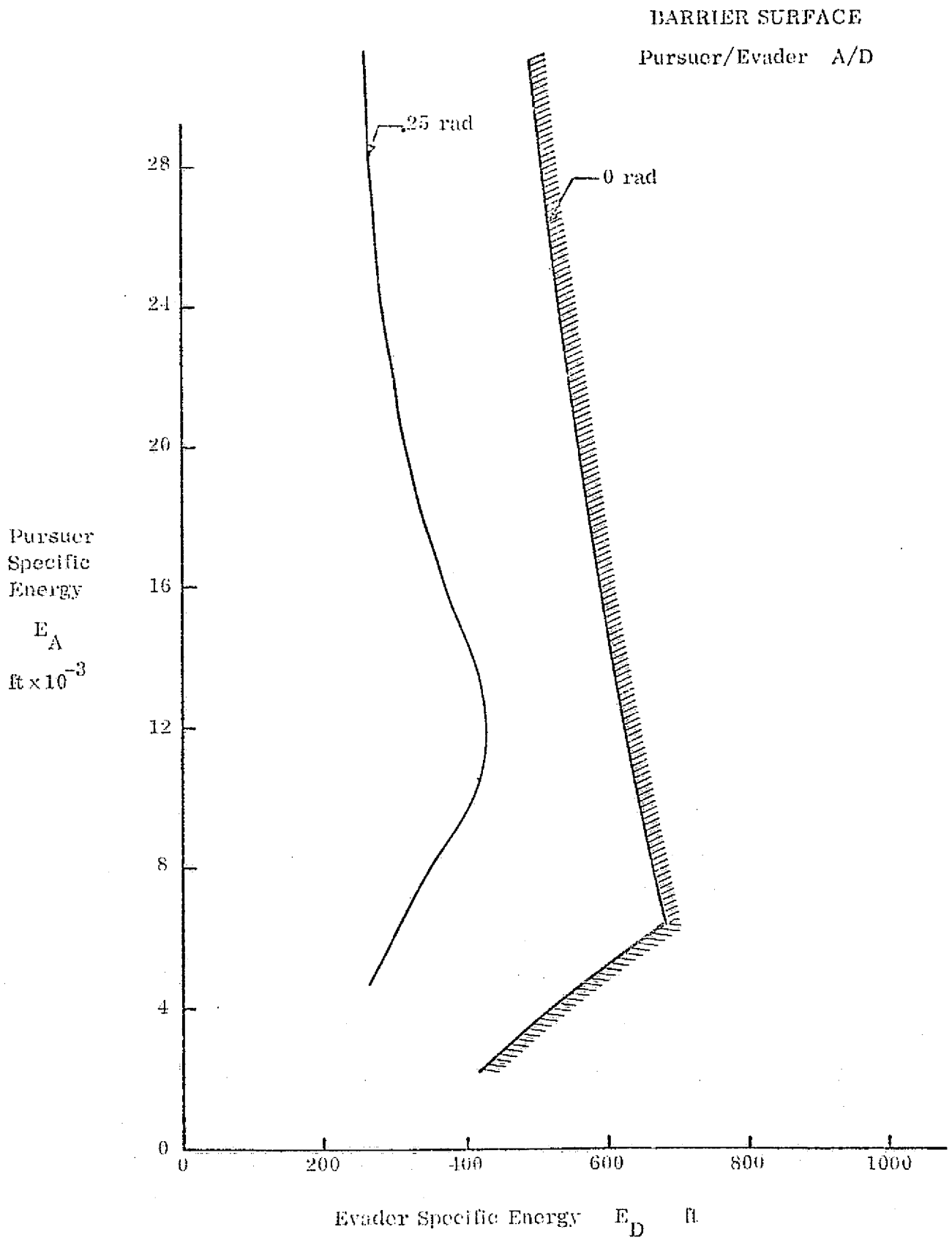
Pursuer/Evader   A/D

FIGURE 14

BARRIER SURFACE

Pursuer/Evader   D/A
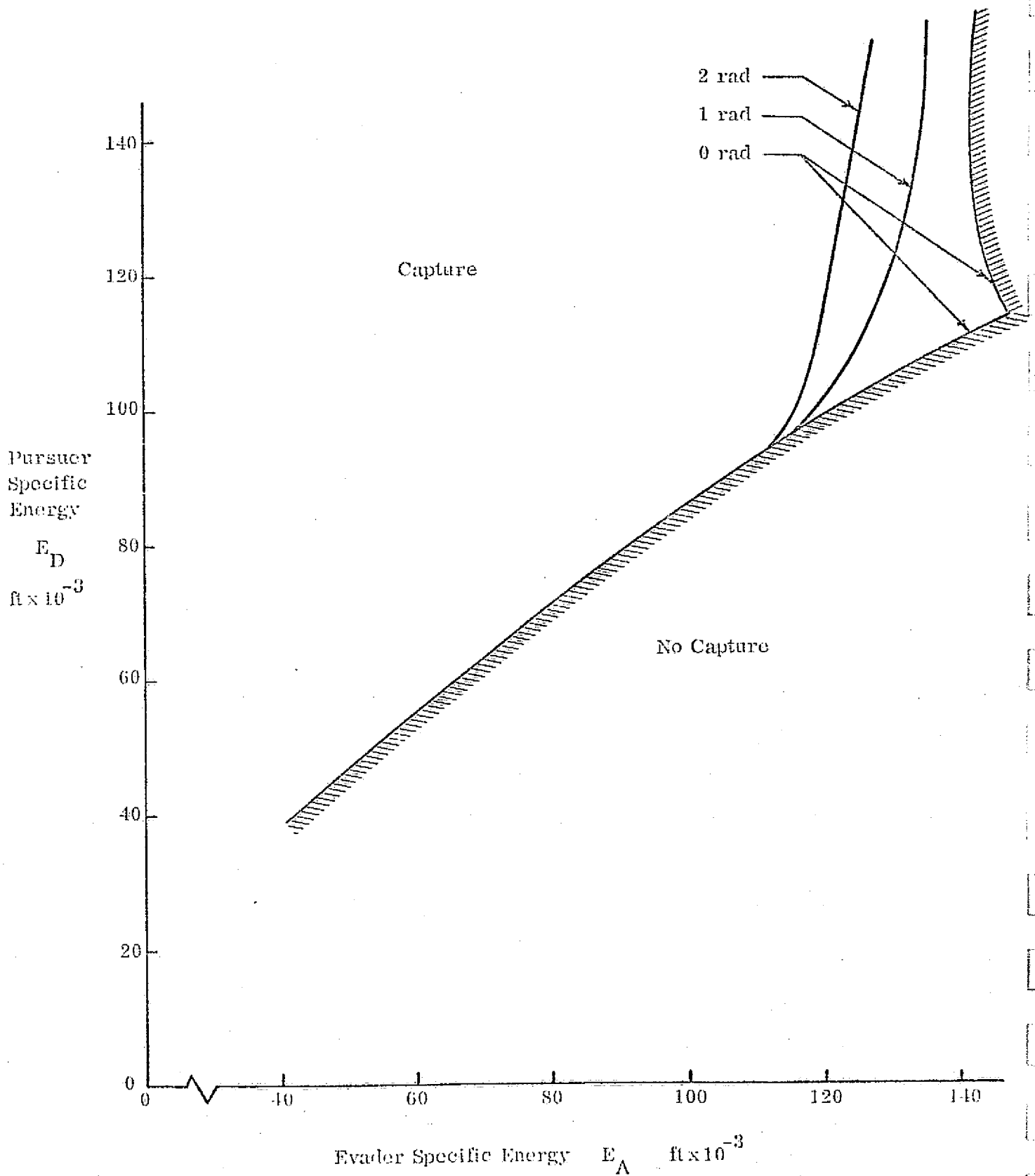
A USER'S GUIDE TO THE

AIRCRAFT ENERGY-TURN AND TANDEM-MOTION

COMPUTER PROGRAMS

Leon Lefton
A. Ralph Krenkel
Henry J. Kelley

Report No. 75-26
Contract NAS 2-8738
June 1975
Revised January 1976

ANALYTICAL MECHANICS ASSOCIATES, INC.
50 JERICHO TURNPIKE
JERICHO, N. Y. 11753

ABSTRACT

This manual is a guide for using the Aircraft Energy-Turn and Tandem Motion programs, digital computer programs for use in differential-turn computations. The program is written in FORTRAN IV for use on a CDC 6600 computer. With slight modification, the program may be run on any digital computer which will accept FORTRAN IV.

The program inputs and outputs are described herein and examples provided. In addition, the program options are discussed and overall flow charts are presented.

The programs described were developed partially under U.S. government contracts: F44620-71-C-0123 with the Asst. Chief of Staff, Studies and Analysis, Headquarters USAF; N00014-73-C-0328 with the Vehicle Warfare Office, Office of Naval Research; and NAS 2-8738 with NASA Ames Research Center.

TABLE OF CONTENTS

LIST OF FIGURES

INTRODUCTION

The Aircraft Energy Turn program is an outgrowth of a digital computer program which was designed to do parameter studies of variable-altitude turns obtained by numerical integration in reduced-order ("energy") approximation for supersonic aircraft, including the effects of constraints on altitude, dynamic pressure, Mach number, lift coefficient, and normal load factor. The general theory of reduced-order approximation for aircraft maneuver optimization is described in Ref. 1. The program described herein provides for the simultaneous integration of two aircraft trajectories, uncoupled except for control of print-out and run termination. The present user's manual overlaps that of Ref. 6, which describes a similar single-aircraft program. It describes, in addition, a related "Tandem-Motion" computer program. The two programs are used in conjunction with a third, "Hodograph", computer program, described in Ref. 7, for differential-turn computations.

The following tables are utilized in the programs: C_{D_o} vs. Mach, $C_{D_{C_L^2}}$ vs. Mach, rho vs. altitude, $\hat{C}_L$ vs. Mach, speed of sound vs. altitude. Thrust tables, which are functions of Mach number and altitude, are also used. Internally, the tables are fit by cubic splines or cubic spline lattices (Ref. 5), with all "moments" (second derivatives at mesh points) stored in tabular form to be used for interpolations during trajectory calculations. The desirable feature of splining for the present application is enhanced smoothness (continuity of second derivatives is maintained), which facilitates the generation of families of solutions of the state/Euler differential equations. The speed brake drag coefficient, C_{D_B}, is introduced as the product of a factor and the zero-lift drag coefficient. A preprocessor is built into the programs so that the user may change any of the tables with input. This is explained in detail in the Input section.

TECHNICAL SUMMARY, ENERGY-TURN PROGRAM

This section summarizes some of the main features of the analytical material presented in Ref. 1. The state variables in the basic system of differential equations are the specific energy, $E \; (= h + V^2/2g)$, and heading angle, χ. The roles of control variables are taken on by altitude, h, bank angle, μ, and throttle setting, $0 \le \eta \le 1$. The Euler system is given by

$$\dot{\lambda}_E = - \partial \tilde{H}/\partial E$$

$$\dot{\lambda}_\chi = - \partial \tilde{H}/\partial \chi$$

The Hamiltonian, H, is given by

$$H \equiv \lambda_E \frac{V(T\eta - D)}{W} + \lambda_\chi \frac{g}{V} \tan \mu$$

The augmented Hamiltonian, $\tilde{H}$, is defined:

$$\tilde{H} = H + \sum_{i=1}^{5} \lambda_i \beta_i$$

where β_i are the inequality constraints:

$$\beta_1 = h - h_T \ge 0 \qquad\qquad \text{terrain limit}$$

$$\beta_2 = \bar{q} - g\rho(E - h) \ge 0 \qquad\qquad \text{dynamic pressure limit}$$

$$\beta_3 = \bar{M} - M \ge 0 \qquad\qquad \text{Mach number limit}$$

$$\beta_4 = \cos \mu - \frac{W/S}{q \bar{C}_L} \ge 0 \qquad\qquad C_{L_{max}} \text{ limit}$$

$$\beta_5 = \cos \mu - \cos \tilde{\mu} \ge 0 \qquad\qquad \text{normal load factor limit}$$

Further details concerning the determination of the multipliers λ_i and the control variables are given in Ref. 1.

It is instructive to consider two basic types of maneuver which are limiting cases. These cases are: (1) symmetric flight, in which the final energy of the aircraft is to be maximized, and (2) hard turning flight, in which the final heading angle is to be maximized regardless of energy loss. The Hamiltonian is a weighted sum of energy and heading rates, namely: $\lambda_E \dot{E}$ and $\lambda_\chi \dot{\chi}$. The program finds the altitude, h, at which the Hamiltonian is a minimum by searching versus h at constant energy level.

The first case, symmetric flight, can be generated by making λ_E negative (say, -1.0) and λ_χ zero or small negative. Because $\dot{\chi}_{max}$ is generally much smaller than $\dot{E}_{max}$ for a given value of E, $\lambda_\chi = -1.0$ is considered a small value. (Actually the multipliers λ_E and λ_χ need be scaled such that $H = -1.0$, but since only the ratio affects the computations, this scaling can be postponed.) A typical trajectory might start with a low energy level, say $E = 5$ to 15,000 feet. With such values, the aircraft executes a generally accelerating, climbing path beginning at sea level, choosing an altitude for which $\dot{E}$ is maximized. Two typical symmetric-flight trajectories are shown in Fig. 1 in an altitude/velocity chart. The trajectories are shown superimposed on the velocity-altitude envelopes corresponding to constant values of $\dot{E}$. Constant energy lines are also shown in the background as in the procedures of Refs. 2 and 3. The aircraft climbs along a path of maximum $\dot{E}$, $(\partial\dot{E}/\partial h)_E = 0$. There is a subsonic and a supersonic branch of the function $(\partial\dot{E}/\partial h)_E = 0$, which overlap in the energy range of approximately $32,500' < E < 45,000'$; i.e., there are two minima. The branch taken depends upon how the search for minimum of H is initiated; in other words, the program does not have the capability of locating a global minimum. The times at which the points along the trajectory are reached, as well as all values of the variables and airplane parameters, are printed at each time-step by the program. See the section labelled Output for further details.

3

FIGURE 1

ALTITUDE/VELOCITY ENVELOPE, BOUNDARIES, AND LOCI
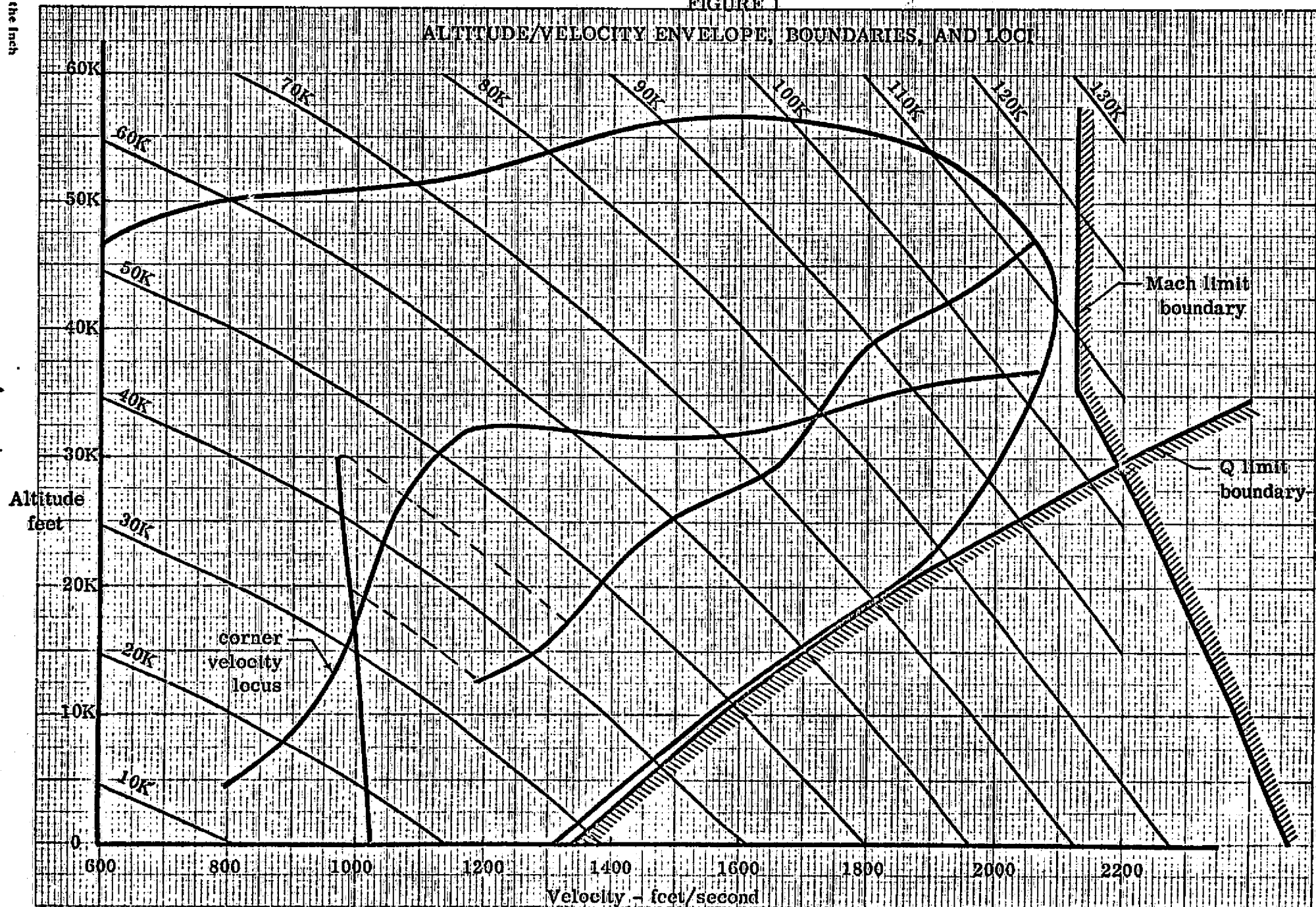
The program does not calculate the altitude-velocity envelope, energy-rate and turn-rate peaks; this is available from the companion "hodograph" program of Ref. 7. Figure 2 presents the peak values of energy rate versus E for the subject aircraft and illustrates the subsonic (first) peak and the supersonic (second) peak. The overlap range is, as noted previously, between $E - 32,500$ and $45,000$. The first trajectory (lower) of Figure 1 transferred from the subsonic to the supersonic branch of constant energy level $E \simeq 34,000$, while the second transferred at $E \simeq 45,000$. The difference in these cases depended upon how the initial altitude iterate was introduced into the 1-D search; selected by ITS=0, where h_{guess} is the minimum of h_1, h_2, and h_3, or by ITS-1, where h_{guess} is the value h calculated in the previous time interval. The second trajectory (upper) required a longer time interval to reach the final energy state than the first, since the first peak was followed for too long. Ideally, the transfer point would occur at the intersection of the first and second peak curves, $E \simeq 36,000$ feet.

The second case of interest is that in which maximum turning rate is sought irrespective of energy rate. In these cases, the Hamiltonian consists of the term $\lambda_X \frac{g}{V} \tan \mu$. Trajectories having this character may be generated by taking λ_X as a very large negative number, of the magnitude: $\lambda_X = -1 \times 10^n$, where $n \geq 8$. The Hamiltonian is minimized when the ratio $(\tan \mu)/V$ is a maximum, and this corresponds to the so-called corner velocity described in Ref. 1, where the load factor as limited by $C_{L_{max}}$ is equal to the maximum allowable load factor of the airframe structure. The corner-velocity locus is not normally generated by the program during a trajectory calculation, but an option is available for executing this calculation.

Figure 1 shows a "corner-velocity" locus in turning flight in the Mach number-altitude plane. As shown in the figure, in the region to the left of the corner velocity,

FIGURE 2

MAXIMA OF $\dot{E}$ vs. E

Symmetric Flight

1st peak

2nd peak

$\dot{E}$

700

600

500

400

300

200

100

0

0   20K   40K   60K   80K   100K   120K

E
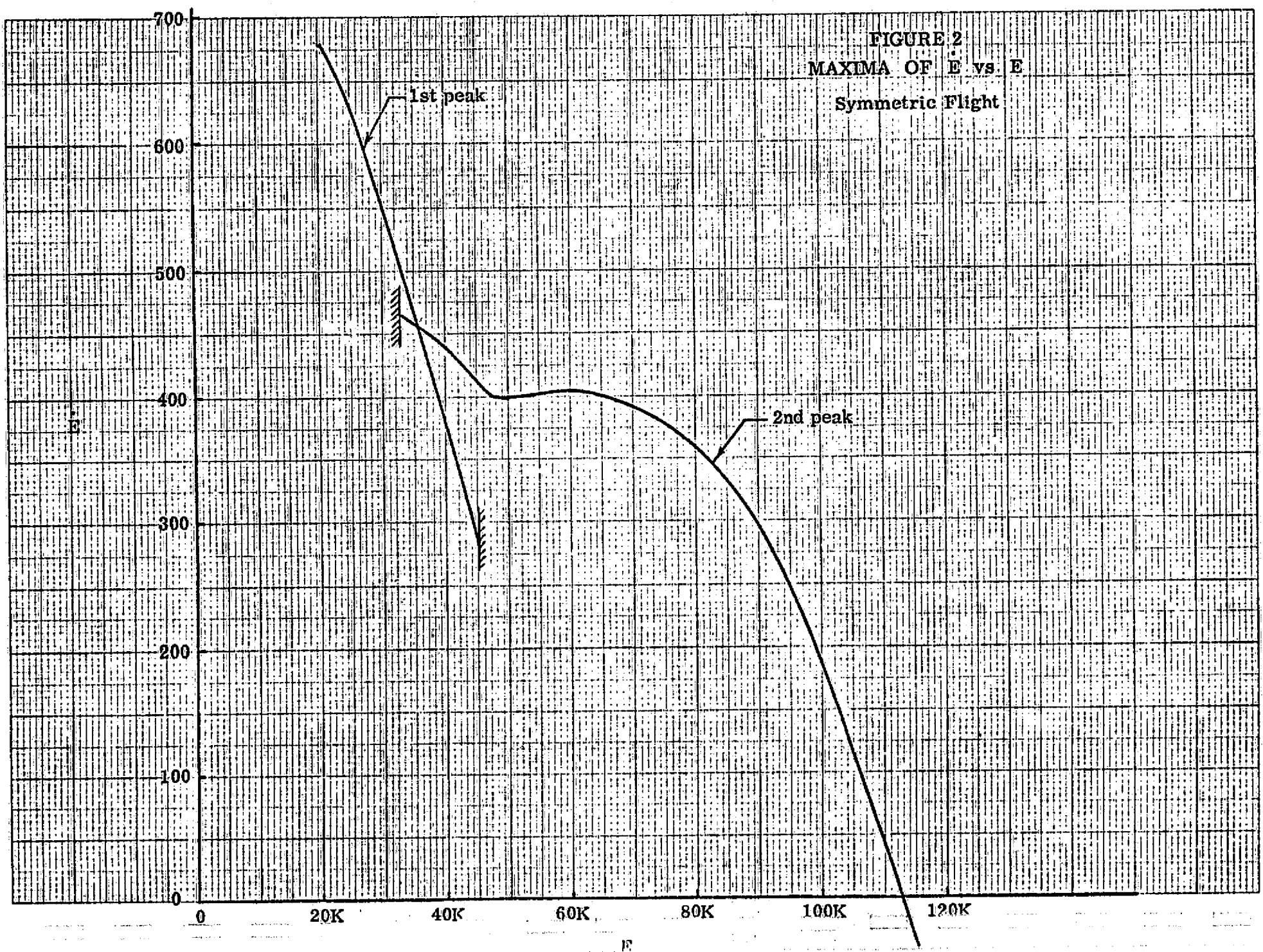
the maneuvering capability of the airplane is limited by $C_{L_{max}}$, while to the right, the structural load factor limits maneuvering.

The general optimal turning maneuver is intermediate between the symmetric energy climb case and the "corner-velocity" case; however, there is more complexity in the general combined turning case than in either of the limiting cases. Thus the Hamiltonian function may exhibit three relative minima versus altitude h at constant energy, and the transition behavior may be quite intricate. Because h, in its appearance as a control variable, is not "the real thing," having arrived by way of an order-reduction approximation, the analyst using the computer program to generate families of Euler solutions may be interested not only in the global minimum of H(h) but in the relative minima as well. Trajectories so generated correspond to so-called "strong" and "weak" extrema, respectively, and complicate the survey of families. Transition between minima should be carefully monitored and controlled by the user constructing families.

The user may elect a mode of operation that provides the global minimum of H(h) and hence "strong" extrema.[1] This is accomplished by a preliminary scan of H values at 500 ft altitude increments over the complete altitude range. While it is computationally expensive, the alternative of controlling transitions off-line is laborious and slow.

Where "weak" minima are of interest, a measure of control over which minimum of the Hamiltonian the program selects is provided the user by two optional input choices described in the next section. One of these permits choice of first guess for the one-dimensional search as either the value of h[2] resulting from the previous 1-D search at the preceding integration step or a value slightly below the minimum altitude limited by terrain, dynamic pressure, or Mach number.[3] A second option

1   ITS = 3

2   ITS = 1

3   ITS = 0

consists of a choice between normal search logic described in Ref. 1, on the one hand, and a logic choosing the minimum altitude[4] whenever the switching function $\lambda_E > 0$ (cut throttle) and the slope $\frac{dH}{dh}$ given by Eq. (123) of Ref. 1 is positive, this restricted (and possibly "weak" minimum) choice reverting to normal logic should either sign change.

A mechanized search for the multiplier value λ_χ yielding a specified energy at a fixed final time is available upon input option. The iterative scheme employed is minimization of the square of the difference in actual and specified final energies via one-dimensional search using golden section and cubic fit techniques of Ref. 4.

The program provides for simultaneous integration of energy and heading-angle histories of two aircraft for convenience in differential-turn computations (Refs. 7 and 8). The computations are independent; however, the print-out interval is controlled in part by turn-angle difference and the integration is terminated on multiple criteria which include violation of prescribed bounds on the specific energy of each craft. The choice between integrating trajectories for one or two aircraft is controlled by input, as discussed in the next section, as is print-out interval and run termination.

For the determination of λ_χ initial values that make the Hamiltonian for the two-vehicle system vanish, hence result in grazing (barrier) trajectories, an iteration procedure is supplied. This minimizes the square of the Hamiltonian via golden-section search.

INPUT SPECIFICATIONS, ENERGY-TURN PROGRAM

A. **Inputs for Preprocessor**

NAMELIST/MINP/ATAB, HATB, CDOT, XMOT, CDCLT, XMCLT,
RHT, HRT, TCLH, YMCL, TRXH, XMTRT, HTRT, NMA, NCDO,
NCDCL, NRH, NCB, NXT, NHT, IDEN, EPSCF, EPSGS, LT

IDEN is dimensioned 6 and each slot is associated with a table ID. The tables are as follows:

ID	Table	Dimension	Number of Points	Description
1	ATAB	20	NMA	a (speed of sound
1	HATB	20	NMA	h (altitude)
2	CDOT	20	NCDO	C_{D_o}
2	XMOT	20	NCDO	Mach No.
3	CDCLT	20	NCDCL	$C_{D_{C_L^2}} = 1/C_{L_\alpha}$
3	XMCLT	20	NCDCL	Mach no.
4	RHT	20	NRH	rho (density)
4	HRT	20	NRH	h
5	TCLH	20	NCB	$\hat{C}_L$
5	YMCL	20	NCB	Mach no.
6	TRXH	20, 20	NXT, NHT	TR (thrust) $\left\{ \begin{array}{l} \text{Mach nos.} = \text{cols.} \\ \text{Altitudes} = \text{rows} \end{array} \right.$
6	XMTRT	20	NXT	Mach no.
6	HTRT	20	NHT	h

If IDEN(7) = 0, the $C_{D_{C_L^2}}$ table is read in directly.

If IDEN(7) $\neq$ 0, the $C_{L_{L_\alpha}}$ table is read into the CDCLT table and the program inverts it before preprocessing.

If all the tables are to be preprocessed, IDEN(I) $\neq$ 0, I = 1, 6.

If the user expects to use the same table or tables for many runs, he may want to avoid the preprocessing by reading in IDEN(I) = 2 on the first run.

9

This will give a printout of the moment table or tables, which may be put into data blocks in the succeeding runs and then IDEN(I) should be set to 0.

LT = 0	Indicates end of run
LT = 1	First aircraft tables are preprocessed
LT = 2	Second aircraft tables are preprocessed
LT = 3	Iterate for minimum $HI(\lambda_\chi)$, $HI(\lambda_\chi) = H_2(\lambda_\chi) - H_1(\lambda_\chi) - H^*$
	See PROG1; Summary of Subroutines
LT = 4	Integrate two-aircraft trajectory
LT = 5	Integrate one-vehicle trajectory only
EPSCF	Epsilon in ONEDIM to measure closeness to origin
EPSGS	Epsilon for convergence tests in above

B. Main Inputs

1. Aircraft One

NAMELIST/MINPUT/GO, H, S, W, E, X, XLE, XLX, TMAX, DELT, EMIN, EB3, HDLT, EPSGS, EPSCF, NEQ, NPRN, IND, INTB, QBAR, QMAX, ICB, DLLME, HSTR, NC, XBAR, XMBAR, XNB, CNCLC, ITS, INCR, HT

Notation Explanation		Units
GO	Gravitational constant (32.16)	ft/sec^2
H	Guess for initial altitude	ft
S	Wing planform reference area	sq ft
W	Weight of aircraft	lbs
E	Initial energy	ft
X	Initial χ angle	rad
XLE	Initial λ_E	
XLX	Initial λ_χ	
TMAX	Maximum time of flight	sec
DELT	Integration interval	sec
EMIN	Trajectory terminates if $E \geq EMIN$	ft

EB3	If $E <$ EB3, bypass β_3 calculation	ft
HDLT	Initial altitude step size for the regular ONEDIM routine	ft
EPSGS	Epsilon for convergence in the golden section of the ONEDIM routine	
EPSCF	Epsilon for closeness to origin	
NEQ	Number of equations to be integrated	
NPRN	Number of integration steps per printout	
IND	Print option indicator (to be explained in the Output section)	
INTB	$0 =$ last case was processed	
	$1 = \beta_{45}$ always calculated	
	$2 = \beta_{45}$ not calculated when $\lambda_E > 0$ and $\partial H/\partial h > 0$	
QBAR	Q boundary for β_2 calculation	
QMAX	Q boundary for cubic fit in ONEDIM routine If $Q >$ QMAX, use cubic fit If $Q \leq$ QMAX, use golden section only	
ICB	$0 - \hat{C}_L = 1$ $1 - \hat{C}_L =$ TCLH (Mach)	
DLLME	First step in ONEDIM on $HI(\lambda_X)$ If initial $\lambda_X = 0$, program will start with $-$DLLME and terminate if it cannot find a minimum If initial $\lambda_X < 0$, program will reverse directions if it cannot find a minimum	
HSTR	$= H^*$	
NC	Number of samples allowed in INEDIM on $HI(\lambda_X)$	
XMBAR	Mach boundary for β_3 calculation	
XNB	n (maximum structural load factor)	
CNCLC	Speed brake factor, where $C_{D_B} =$ CNCLC $* C_{D_0}$	
ITS	First guess for altitude in 1-D search $0 -$ taken from previous β_1, β_2, or β_3 solution $- 500. - .2*E$ $1 -$ taken from previous 1-D search $3 -$ scans an altitude range for minimum Hamiltonian	

INCR	Number of steps in scan mode	
HT	Maximum altitude allowed	ft.
XBAR	If $\chi_1 - \chi_2 \geq$ XBAR, trajectory terminates	rad

2. Aircraft Two

NAMELIST/MINP2/H, X, W, E, XLE, XLX, EB3, HDLT, XNB, INTB, QBAR, QMAX, ICB, XMBAR, CNCLC, ITS, INCR, HT, S, IND, EMIN

See above for explanation.

C. ERROR CODES

Printout Number	Location
40	Table look-up
100	Scan mode: lower limit exceeds upper limit
111	Aircraft 1: $h > E$
112	Aircraft 1: $\cos \mu^* > 1$
121	Aircraft 2: $h > E$
122	Aircraft 2: $\cos \mu^* > 1$
334	Subroutine SPINT: Interpolation for $\lambda_E = 0$

D. Sample Input

Two-Vehicle trajectory: Aircraft One   F-5
                         Aircraft Two   F-4

```
$MINP
LT=2,
NMA=20,
ATAB=1496.,1116.,1097.,1077.,1057.,1037.,1016.,994.7,968.1,968.1,958.1,
968.1,958.1,968.1,968.1,958.1,956.1,984.2,1004.,1056.43,
HATB=-1.E5,0.,5.E3,1.E4,1.5E4,2.E4,2.5E4,3.E4,3.609E4,4.E4,4.5E4,5.E4,
5.5E4,6.E4,7.E4,8.E4,8.202E4,9.E4,1.E5,2.E5,
NRH=20,
RHT=6821.E-5,2377.E-6,2043.E-5,1765.E-6,1496.E-,,1266.E-6,1065.F-5,
8893.E-7,7001.E-7,5951.E-7,4601.E-7,3618.F-7,2845.E-7,2236.E-7,
1384.E-7,8556.E-8,7764.E-8,5151.E-8,3131.E-8,94.E-8,
HRT=-1.E6,0.,5.E3,1.E4,1.5E4,2.C4,2.5E4,3.E4,3.609E4,4.E4,4.5E4,5.E4,
5.5E4,6.E4,7.E4,8.E4,8.202E4,9.E4,1.E5,2.E5,
NCDO=19,
CDOT=.0205,.0205,.0205,.0205,.0205,.0210,.0213,.0242,.0324,.0359,.0374,.0344,
.0385,.0385,.0387,.0397,.0403,.0403,.0403,0.,
XMOT=0.,.2,.65,.75,.80,.85,.90,.95,1.00,1.05,1.10,1.20,1.40,1.60,1.80,2.,
2.2,2.4,2.6,0.,
NCB=14,
XMCLT=0.,.2,.65,.75,.80,.85,.90,.95,1.0,1.05,1.10,1.20,1.40,1.60,1.80,2.,
2.2,2.4,2.6,0.,
NCDCL=19,
CDCLT=.198,.198,.198,.201,.205,.211,.218,.228,.230,.252,.265,.297,.368,.453,
.544,.64,.744,.744,.744,0.,
YMCL=0.,.1,.3,.5,.7,.9,1.1,1.3,1.5,1.7,1.9,2.1,2.3,2.6,0.,0.,0.,0.,0.,
TCLH=.85,.85,.83,.81,.74,.68,.90,.75,.54,.45,.40,.35,.30,.3,
0.,0.,0.,0.,0.,0.,
NXT=14,NHT=10,
XMTRT=0.,.2,.4,.6,.8,1.,1.2,1.4,1.6,1.8,2.,2.2,2.4,2.6,0.,0.,0.,0.,0.,0.,
HTRT=-100000.,0.,10000.,20000.,30000.,40000.,50000.,60000.,70000.,
200000.,0.,0.,0.,0.,0.,0.,0.,0.,0.,0.,
TRXH(1,1)=120200.,120200.,117400.,108800.,119200.,102000.,33400.,2200.,9600.,
5600.,5600.,5600.,5600.,5600.,0.,0.,0.,0.,0.,0.,
TRXH(1,2)=32200.,32200.,33400.,34600.,39200.,42000.,41400.,40200.,39600.,
39600.,39600.,39600.,39600.,39600.,0.,0.,0.,0.,0.,0.,
TRXH(1,3)=23400.,23400.,25000.,27400.,31200.,35000.,42200.,44000.,43000.,
42000.,42000.,42000.,42000.,42000.,0.,0.,0.,0.,0.,0.,
TRXH(1,4)=16400.,16400.,17200.,19700.,23200.,27500.,32600.,38000.,42400.,
44800.,43000.,43000.,43000.,43000.,0.,0.,0.,0.,0.,0.,
TRXH(1,5)=11000.,11000.,11600.,13200.,15000.,19500.,24000.,28600.,33200.,
37200.,38500.,37800.,36000.,36000.,0.,0.,0.,0.,0.,0.,
TRXH(1,6)=6600.,6600.,7200.,8200.,10000.,12600.,15800.,19400.,23000.,
26400.,28400.,28600.,26000.,20400.,0.,0.,0.,0.,0.,0.,
TRXH(1,7)=4200.,4200.,4400.,5000.,5300.,7600.,9400.,11600.,14000.,16200.,
17600.,17300.,15400.,12800.,0.,0.,0.,0.,0.,0.,
TRXH(1,8)=2600.,2600.,2800.,3200.,3800.,4500.,5600.,7000.,8400.,9800.,
10600.,10800.,13200.,7500.,0.,0.,0.,0.,0.,0.,
TRXH(1,9)=2000.,2000.,2000.,2200.,2400.,2400.,3400.,4000.,4800.,5500.,
6200.,5400.,6000.,4600.,0.,0.,0.,0.,0.,0.,
TRXH(1,10)=20*0.,
IDEN=1,1,1,1,1,1,0,
$END
```

13

```
$MINP
LT=1,
NMA=20,
ATAB=1496.,1116.,1097.,1077.,1057.,1037.,1016.,994.7,968.1,968.1,968.1,
968.1,968.1,968.1,968.1,958.1,958.1,984.2,1004.,1056.45,
HATB=-1.E5,0.,5.E3,1.E4,1.5E4,2.E4,2.5E4,3.E4,3.609E4,4.E4,4.5E4,5.E4,
5.5E4,6.E4,7.E4,8.E4,8.202E4,9.E4,1.E5,2.E5,
NRH=20,
RHT=6821.E-5,2377.E-6,2048.E-6,1755.E-6,1496.E-6,1266.E-6,1065.E-6,
8893.E-7,7061.E-7,5851.E-7,4601.E-7,3618.E-7,2845.E-7,2238.E-7,
1384.E-7,8556.E-8,7764.E-8,5151.E-8,3131.E-8,94.E-8,
HRT=-1.E5,0.,5.E3,1.E4,1.5E4,2.E4,2.5E4,3.E4,3.609E4,4.E4,4.5E4,5.E4,
5.5E4,6.E4,7.E4,8.E4,8.202E4,9.E4,1.E5,2.E5,
NCB=16,
YMCL=0.,.2,.4,.5,.7,.8,.9,.95,1.,1.05,1.1,1.2,1.4,1.6,1.8,3.,4*0.,
TCLH=.86,.86,.86,.79,.76,.74,.84,1.04,1.2,1.27,1.28,1.13,.85,.65,.5,.5,
4*0.,
NCDO=16,
XMOT=0.,.2,.4,.6,.7,.8,.9,.95,1.,1.05,1.1,1.2,1.4,1.6,1.8,3.,4*0.,
CDOT=.02,.02,.0195,.0192,.0183,.0189,.0203,.027,.038,.0408,.0406,.0409,
.0414,.0413,.0413,.0413,4*0.,
NCDCL=16,
XMCLT=0.,.2,.4,.6,.7,.8,.9,.95,1.,1.05,1.1,1.2,1.4,1.6,1.8,3.,4*0.,
CDCLT=6.4,6.4,6.4,6.4,6.6,7.6,7.1,6.6,6.5,6.4,5.3,4.6,3.8,3.,2.5,2.5,4*0.,
NXT=10,NHT=9,
XMTRT=0.,.2,.4,.5,.8,1.,1.2,1.4,1.6,1.8,10*0.,
HTRT=-15000.,0.,15000.,25000.,36089.,40000.,45000.,50000.,175000.,11*0.,
TRXH(1,1)=9100.,9100.,9900.,10700.,11500.,12100.,13200.,14300.,15400.,
16500.,10*0.,
TRXH(1,2)=6600.,6600.,7200.,7900.,8700.,9500.,10300.,11100.,11900.,
12700.,10*0.,
TRXH(1,3)=4100.,4100.,4500.,5100.,5900.,6900.,7400.,7900.,8400.,8900.,
10*0.,
TRXH(1,4)=2500.,2500.,3000.,3500.,4100.,5000.,6000.,6900.,7800.,8700.,
10*0.,
TRXH(1,5)=1000.,1000.,1600.,2200.,2600.,3300.,4100.,4800.,5400.,5900.,
10*0.,
TRXH(1,6)=700.,700.,1200.,1700.,2200.,2800.,3400.,4000.,4600.,5200.,10*0.,
TRXH(1,7)=800.,800.,1100.,1400.,1700.,2100.,2700.,3200.,3700.,4200.,10*0.,
TRXH(1,8)=600.,600.,700.,1000.,1300.,1600.,2000.,2400.,2800.,3200.,10*0.,
TRXH(1,9)=20*0.,
IDEN=1,1,1,1,1,1,1,
$END
```

```
$MINP
EPSF=1.E-5,EPSGS=1.E-5,
LT=4,
$END
$MINPUT
GO=32.2,H=10000.,S=170.,W=13000.,C=40000.,XLE=-1.,XLX=-1.,
TMAX=200.,DELT=-1.,
QBAR=4000.,ICB=0,XNB=6.7891,XMBAR=3.,CNCLC=1.5,INT3=1,EB3=180000.,
ITS=3,HOLT=10.,QMAX=170000.,INCR=500,EMIN=80000.0,EPSGS=.1E-10,
W=9545.,XNB=7.33,QBAR=1700.,XMBAR=1.72,
EPSCF=.1E-10,IND=1,NPRN=5,NEQ=5,HI=0.,
XBAR=5.,
XLX=-1.,
E=18500.,XLE=-.1E-7,XLX=-1.,
$END
$MINP2
S=530.,W=37523.,X=0.,INCR=500,CNCLC=1.,QBAR=2167.325,XMBAR=2.2,
XNB=7.,ICB=1,H=25000.,ITS=3,INT3=1,HOLT=50.,
EB3=180000.,
XLE=-2.80607750143147,E=67395.7855486957,QMAX=2300.,
XLX=-.47656320157254E5,EMIN=120000.,
E=7500.0,XLE=-.1E-7,XLX=-1.,
IND=1,
$END
$MINPUT
INT3=0,
$END
$MINP
LT=3,
$END
```

ORIGINAL PAGE IS
OF POOR QUALITY

Sample input for a two-vehicle iteration followed by a trajectory:

```
$HIMP
LI=2,
NMA=20,
ATAB=1436.,1115.,1097.,1077.,1057.,1037.,1016.,994.7,958.1,958.1,958.1,
968.1,958.1,958.1,958.1,958.1,958.1,958.1,984.2,1004.,1056.43,
HATB=-1.E5,0.,5.E3,1.E4,1.5E4,2.E4,2.5E4,3.E4,3.609E4,4.E4,4.5E4,5.E4,
5.5E4,6.E4,7.E4,8.E4,8.202E4,9.E4,1.E5,2.E5,
NRH=20,
RHT=5821.E-6,2377.E-6,2043.E-6,1755.E-6,1496.E-6,1266.E-6,1065.E-6,
8393.E-7,7061.E-7,5351.E-7,4601.E-7,3618.F-7,2845.E-7,2238.E-7,
1384.E-7,8556.E-8,7764.E-8,5151.E-8,3131.E-8,94.E-8,
HRT=-1.E6,0.,5.E3,1.E4,1.5E4,2.E4,2.5E4,3.E4,3.609E4,4.E4,4.5E4,5.E4,
5.5E4,6.E4,7.E4,8.E4,8.202E4,9.E4,1.E5,2.E5,
NCDD=19,
CDOT=.0205,.0205,.0205,.0205,.0205,.0210,.0210,.0242,.0324,.0359,.0374,.0384,
.0385,.0385,.0387,.0397,.0403,.0403,.0403,0.,
XMDT=0.,.2,.65,.75,.80,.85,.90,.95,1.00,1.05,1.10,1.20,1.40,1.60,1.80,2.,
2.2,2.4,2.6,0.,
NCD=14,
XMDLT=0.,.2,.65,.75,.80,.85,.90,.95,1.0,1.05,1.10,1.20,1.40,1.60,1.80,2.,
2.2,2.4,2.6,0.,
NCDDL=13,
CDDLT=.198,.198,.198,.201,.205,.211,.218,.228,.239,.252,.265,.297,.368,.453,
.544,.64,.744,.744,.744,0.,
YMDL=0.,.1,.3,.5,.7,.9,1.1,1.3,1.5,1.7,1.9,2.1,2.3,2.6,0.,0.,0.,0.,0.,0.,
TCLH=.85,.85,.83,.81,.73,.68,.90,.75,.54,.45,.40,.35,.30,.3,
0.,0.,0.,0.,0.,0.,
NXT=14,NHT=10,
XHTRT=0.,.2,.4,.6,.8,1.,1.2,1.4,1.6,1.8,2.,2.2,2.4,2.6,0.,0.,0.,0.,0.,0.,
HTRT=-100000.,0.,10000.,20000.,30000.,40000.,50000.,60000.,70000.,
200000.,0.,0.,0.,0.,0.,0.,0.,0.,0.,0.,
TRXH(1,1)=120200.,120200.,117400.,108800.,119200.,102000.,33400.,2200.,5600.,
5600.,5600.,5600.,5600.,5600.,0.,0.,0.,0.,0.,0.,
TRXH(1,2)=32200.,32200.,33400.,34800.,39200.,42000.,41400.,40200.,39600.,
39500.,39500.,39500.,39500.,39500.,0.,0.,0.,0.,0.,0.,
TRXH(1,3)=23400.,23400.,25000.,27400.,31200.,36000.,42200.,44000.,43000.,
42000.,42000.,42000.,42000.,42000.,0.,0.,0.,0.,0.,0.,
TRXH(1,4)=16400.,16400.,17200.,19600.,23200.,27600.,32600.,38000.,42400.,
44800.,43000.,43000.,43000.,43000.,0.,0.,0.,0.,0.,0.,
TRXH(1,5)=11000.,11000.,11500.,13200.,16000.,19600.,24000.,28600.,33200.,
37200.,38600.,37800.,36300.,35000.,0.,0.,0.,0.,0.,0.,
TRXH(1,6)=6600.,6600.,7200.,8200.,10000.,12600.,15800.,19400.,23000.,
26400.,28400.,28600.,26000.,20400.,0.,0.,0.,0.,0.,0.,
TRXH(1,7)=4200.,4200.,4400.,5300.,5800.,7500.,9400.,11600.,14000.,16200.,
17500.,17800.,16400.,12300.,0.,0.,0.,0.,0.,0.,
TRXH(1,8)=2600.,2600.,2800.,3100.,3500.,4600.,5600.,7000.,8400.,9800.,
10600.,10800.,10200.,7500.,0.,0.,0.,0.,0.,0.,
TRXH(1,9)=2000.,2000.,2000.,2200.,2400.,2800.,3400.,4000.,4800.,5600.,
6200.,6400.,6000.,4600.,0.,0.,0.,0.,0.,0.,
TRXH(1,10)=20*0.,
IDEN=1,1,1,1,1,1,0,
$END
```

16

```
ININP
LT=1,
NMA=20,
ATAB=1496.,1116.,1097.,1077.,1057.,1037.,1015.,994.7,968.1,968.1,958.1,
958.1,968.1,958.1,958.1,908.1,966.1,984.2,1104.,1156.43,
HATB=-1.E5,0.,5.E3,1.E4,1.5F4,2.E4,2.5E4,3.E4,3.603E4,4.E4,4.5E4,5.E4,
5.5E4,6.E4,7.E4,8.E4,8.20?E4,9.E4,1.E5,2.E5,
NRH=20,
RHT=6821.E-5,2377.E-6,2040.E-6,1705.E-6,1496.E-6,1266.E-6,1065.E-6,
8893.E-7,7061.E-7,5351.E-7,4601.E-7,3618.E-7,2845.E-7,2238.E-7,
1384.E-7,8556.E-8,7764.E-8,5151.E-8,3131.E-8,94.E-8,
HRT=-1.E5,0.,5.E3,1.E4,1.5E4,2.E4,2.5E4,3.E4,3.609E4,4.E4,4.5E4,5.E4,
5.5E4,6.E4,7.E4,8.E4,8.20?E4,9.E4,1.E5,2.E5,
NCB=16,
YMCL=0.,.2,.4,.6,.7,.8,.9,.95,1.,1.05,1.1,1.2,1.4,1.6,1.8,3.,4*0.,
TCLH=.85,.96,.86,.79,.75,.74,.84,1.04,1.2,1.27,1.29,1.13,.86,.55,.5,.5,
4*0.,
NCOO=16,
XHOT=0.,.2,.4,.6,.7,.8,.9,.95,1.,1.05,1.1,1.2,1.4,1.6,1.8,3.,4*0.,
COOT=.02,.02,.0195,.0192,.0188,.0189,.0203,.027,.038,.0408,.0406,.0409,
.0414,.0413,.0413,.0413,4*0.,
NCOOL=16,
XMOLT=0.,.2,.4,.6,.7,.8,.9,.93,1.,1.05,1.1,1.2,1.4,1.6,1.8,3.,4*0.,
COOLT=6.4,6.4,6.4,6.4,6.6,7.6,7.1,5.6,6.5,6.4,5.3,4.6,3.8,3.,2.5,2.5,4*0.,
NXT=10,NHT=9,
XHTRT=0.,.2,.4,.6,.8,1.,1.2,1.4,1.6,1.8,10*0.,
HTRT=-15000.,0.,15000.,25000.,35089.,40000.,45000.,50000.,175000.,11*0.,
TRXH(1,1)=9100.,9100.,9900.,10700.,11500.,12100.,13200.,14300.,15400.,
15500.,10*0.,
TRXH(1,2)=6600.,6600.,7200.,7900.,8700.,9500.,10300.,11100.,11900.,
12700.,10*0.,
TRXH(1,3)=4100.,4100.,4500.,5100.,5900.,6900.,7400.,7900.,8400.,8900.,
10*0.,
TRXH(1,4)=2500.,2500.,3000.,3500.,4100.,5000.,6000.,6900.,7800.,8700.,
10*0.,
TRXH(1,5)=1000.,1000.,1600.,2200.,2600.,3500.,4100.,4800.,5400.,5900.,
10*0.,
TRXH(1,6)=750.,700.,1200.,1700.,2000.,2800.,3400.,4000.,4600.,5200.,10*0.,
TRXH(1,7)=800.,800.,1100.,1400.,1700.,2100.,2700.,3200.,3700.,4200.,10*0.,
TRXH(1,8)=500.,500.,700.,1000.,1300.,1600.,2000.,2400.,2800.,3200.,10*0.,
TRXH(1,9)=20*0.,
IDEN=1,1,1,1,1,1,1,
$END
```

```
$MINP
EPSF=1.E-5,EPSGS=1.E-5,
LT=3,
$END
$MINPUT
GO=32.2,H=10000.,S=170.,W=13000.,E=40000.,XLE=-1.,XLX=-1.,
TMAX=200.,DELT=-1.,
QBAR=4000.,ICB=0,XNB=6.7831,XMBAR=3.,CNCLC=1.5,INTB=1,EB3=180000.,
ITS=3,HOLT=10.,QMAX=170000.,INCR=500,EMIN=80000.0,EPSGS=.1E-10,
W=9545.,XNB=7.33,QBAR=1700.,XMBAR=1.72,
EPSCF=.1E-10,IND=1,NPRN=5,NEQ=6,HT=0.,
XBAR=5.,
NC=30,
DLLME=10000.,XLX=0.,E=200.,XLE=-.9750007,
$END
$MINP2
S=530.,W=37523.,X=0.,INCR=500,CNCLC=1.,QBAR=2157.325,XMBAR=2.2,
XNB=7.,ICB=1,H=25000.,ITS=3,INTB=1,HOLT=50.,
EB3=180000.,
XLE=-2.30607750143147,E=67395.7853486957,QMAX=2300.,
XLX=-.47656820167254E5,EMIN=120000.,
XLX=0.,E=2262.727,XLE=-.9431427,
IND=1,
$END
$MINPUT
INTB=0,
$END
$MINP
LT=4,
$END
$MINPUT
INTB=1,
$END
$MINP2
$END
$MINPUT
INTB=0,
$END
$MINP
LT=0,
$END
```

OUTPUT, ENERGY-TURN PROGRAM

Time history of a trajectory.

1. **Aircraft One**

   IND = 1   Normal printout at print times, TMAX, and whenever ETA changes.

   Time, T, in seconds from T_o; energy; χ angle in radians; λ_E; λ_χ; altitude; velocity; Q; Mach No.; tan μ; ρ(density); thrust; HM (altitude from ONEDIM; HPRM (Hamiltonian); XDIF ($\chi_1 - \chi_2$); $\dot{E}$; $\dot{\chi}$; $\dot{\lambda}_E$; $\dot{\lambda}_\chi$; ETA; A; PDV

   IND = 2   Additional printout for debugging purposes (see PRINT subroutine)

2. **Aircraft Two**

   Same as for Aircraft One but without XDIF.

   ### Output Notation

   When IND $\neq$ 1, output is

T	=	time in seconds from T_o
E	=	energy
X	=	χ in radians
LME	=	λ_E
LMX	=	λ_χ
ALT	=	altitude
V	=	velocity
Q	=	q ($\frac{1}{2}\rho V^2$)

19

M	=	Mach number
TANU	=	tangent μ
RHO	=	ρ
TR	=	thrust
HM	=	altitude from 1-D search
HPRM	=	augmented Hamiltonian
D	=	drag
L	=	lift
SINU	=	sine μ
COSU	=	cosine μ
CDO	=	zero lift drag coefficient
CDB	=	speed brake drag coefficient
CLB	=	$C_{L_{max}}$ or $C_L = \dfrac{nW}{Sg}$
CDCL2	=	induced drag factor
HH	=	augmented Hamiltonian for first guess of 1-D search
PHRH	=	$\partial\rho/\partial h$
PAH	=	$\partial a/\partial h$
PTH	=	$\partial TR/\partial h$
PTE	=	$\partial TR/\partial E$
EDOT	=	$\dot{E}$
XDOT	=	$\dot{X}$

XLED	$=$	$\dot{\lambda}_E$
XLXD	$=$	$\dot{\lambda}_X$
ETA	$=$	η
A	$=$	speed of sound
PDV	$=$	$\partial D / \partial V$
PCDOM	$=$	$\partial C_{D_0} / \partial M$
PCDBM	$=$	$\partial C_{D_B} / \partial M$
PCDCM	$=$	$\partial C_{D_{C_L^2}} / \partial M$
PCLBM	$=$	$\partial \bar{C}_L / \partial M$
B(1-5)	$=$	$\beta (1-5)$
HH1	$=$	augmented Hamiltonian from 1-D search
HH2	$=$	augmented Hamiltonian on $\beta_{4,5}$ boundary
HH3	$=$	augmented Hamiltonian on $\beta_{1,2,\text{or}3}$ boundary
EXTRA	$=$	extra term in $\dot{\lambda}_E$ equation
HMZ	$=$	H on $\beta_{1,2,\text{or}3}$ boundary
HMQ	$=$	H on $\beta_{4,5}$ boundary
PHU	$=$	$\partial H / \partial \mu$
PHH	$=$	$\partial H / \partial h$
IJK	$=$	indicator for boundaries

$1 \ = \ \beta_1$ boundary

$2 \ = \ \beta_2$ boundary

$3 \ = \ \beta_3$ boundary

$4 \ = \ \beta_{4,5}$ boundary

$5 \ = $ 1-D search

SAMPLE JOB SETUP, ENERGY-TURN PROGRAM

Setup for CDC 6600

All control card punches start in Column 1.

ID12345, CM75000, T300.	ID No., amount of core to be used, total running time.
RUN(S)	Set to run.
SET(0)	Sets core to 0.
LGO/RFL, LL=777777/.	Will allow additional lines of output to be printed, over and above normal job cut-off.
7 8 9	End of record.
Source Deck	
7 8 9	End of record.
Data	
6 7 8 9	End of file.

SUMMARY OF SUBROUTINES, ENERGY-TURN PROGRAM

MANE
Main Program
Calls PREPR

PREPR

Reads input.
Preprocesses when necessary.
Calls PROG or PROG1
Calls EXIT

BLOCK DATA

Contains data common to the entire program.

DBLSPL

Called by PREPR
Calculates moments to be used in spline fits for thrust and
  partials of thrust with respect to altitude and energy.

DERIV

Called by PROG and RKCAL
Calculates derivatives for equations to be integrated for Aircraft One.

DERIV2

Called by DERIV
Calculates derivatives for equations to be integrated for Aircraft Two.

ERROR

Called from various parts of program, namely:

FNDIX	–	ID No. 40
FNDHM	–	" I
FNALT	–	" 100
SLF	–	" 111 or 112
SLF2	–	" 121 or 122
SPINT	–	" 334

Writes ID No. for error location.
Calls PRINT
Goes to next case.

FINDH(H1)

Called by DERIV
Finds the altitude as a function of λ_E, λ_χ, E.

FINDH2(H2)

        Called by DERIV2

FNALT

        Called by FINDH
        Used when ITS = 3 .
        Scans altitude range for minimum Hamiltonian and chooses
          proper boundary to follow.

FNALT2

        Called by FINDH2

FNDHM(E)

        Called by FINDH
        Finds altitudes which cause β_1, β_2, β_3, and $\beta_{4,5}$ to go to zero
          and chooses the desired altitude.

FNDHM2(E2)

        Called by FINDH2

FNDIX(IX, N, X, XTB)

        Called by FNDHM and NCALC
        Finds upper index IX for an interval in an N point table XTB
          within which X falls.

INPUT

        Called by PREPR
        Reads input by means of namelist for Aircraft One.

INPUT2

        Called by INPUT
        Reads input for Aircraft Two.

MATIN(A, N, B, M, KEY, DETERM)

        Called by DBLSPL, SNGSPL, ONED, and ONEDIM
        Solves the system $Ax = B$.
        A is an $n \times n$ matrix, B is an n-vector.
        Answer X covers up B, and A is altered.
        Method used is a double-pivoting Gaussian elimination.
        If KEY $\neq$ N , matrix is singular.
        DETERM contains determinant of A .

NCALC

Called by SLF
Finds thrust (TR), $\partial TR/\partial h$, $\partial TR/\partial E$, A, $\partial A/\partial h$, CDO, $\partial CDO/\partial M$, CDCL2, $\partial CDCL2/\partial M$, ρ, $\partial \rho/\partial h$, $\overline{CD}$, $\partial \overline{CD}/\partial M$, $\hat{CL}$, and $\partial \hat{CL}/\partial M$ by using cubic splines.

NCALC2

Called by SLF2

ONED(ITT, NTAPE, CAYMIN, EX1, MPTS, 0, CCAY)
ITT   – Counter for number of function evaluations
NTAPE   – Output tape number
CAYMIN   – Answer
EX1   – First guess
MPTS   = 4
CCAY   – Initial step size (Δx)

Called by PROG1
Finds x for minimum F, where F = f(x) evaluated by
SLFX(F, EX(1)).
This routine is used to find the λ_χ which will find minimum
$$HI(\lambda_\chi)^2 = (H_2(\lambda_\chi) - H_1(\lambda_\chi) - H^*)^2.$$

ONEDIM(ITT, NTAPE, CAMIN, EX1, MPTS, 0, CCAY)
Called by FINDH
Same as above, except this subroutine is used to find h for
minimum Hamiltonian where H = f(h).
Calls SLFUN(F, EX(1)) instead of SLFX(F, EX(1)).

PRINT

Called by PROG and ERROR
Prints out for Aircraft One as explained in the Output section.

PRINT2

Called by PRINT
Prints output for Aircraft Two.

PROG

Called by PREPR
Calculates a trajectory from T = 0 to T = TMAX or from
T = TMAX to T = 0 depending upon DELT.
DELT > 0   forward
DELT < 0   backward

PROG1

Called by PREPR

Sets up a table of 9 λ_X's, starting with $\lambda_{X_1} = 0$.

Does a scan of $HI(\lambda_{X_i})$; whenever $HI(\lambda_{X_i})$ changes sign, λ_X for $HI(\lambda_X) = 0$ is estimated by linear interpolation and the estimate is used as a first guess for a ONEDIM search on $(HI(\lambda_X))^2$. The first two crossings are recorded and, for each solution of λ_X obtained, a trajectory is run.

Inputs needed for these iterations that result from computations in the hodograph program are:

Evader

XLE	- PAR-LFT-CEIL TO ENERGY
E	SPECIFIC ENERGY
XLX	CORNER MULT RATIO-EV

Pursuer

XLE	- PAR-LF-CE-PUR TO ENERGY	From Loft-Ceiling Matched Rates Table
E	PUR-EN MATCHED	
XLX	CORNER MULT RATIO-PUR	

RKCAL(ID)

Called by PROG and PREPR

This is a fourth-order Runge-Kutta integrator with a round-off control.

ID = 1 Initializes the routine. Calculates coefficients to the full capacity of the computer.

ID = 2 Normal integration step.

ID = 3 Restart - Q block is zeroed out (round-off control).

SLF

Called by SLFUN, FINDH, FNDHM, and FNALT

SLF2

Called by SLFUN, FINDH2, FNDHM2, and FNALT2

SLFUN (HH, RR)

> Called by ONEDIM
> Evaluates HH where $HH = f(h + RR * RDL)$.
> h is in COMMON.
> $RDL = +1$ or -1 and is also in COMMON.
> $\partial H / \partial h$ and $\partial H / \partial \mu$ are also calculated when $RR = 0$.
> As a by-product, we also get TANU, SECU, COSU, SINU,
>   D, and TR.

SLFX(F, X)

> Called by ONED
> Evaluates $F = f(x) = (H2 - H1 - H^*)^2$.
> $X = \lambda_\chi$

SPINT

> Called by PROG
> Interpolates for $\lambda_\chi = 0$.

SPLINE

> Called by NCALC
> Computes cubic spline fits for various tables.

SPLN

> Called by NCALC
> Computes cubic spline fits for double table look-ups.

SNGSPL

> Called by PREPR
> Calculates moments to be used in computing cubic spline fits
>   later in the program.

TECHNICAL SUMMARY, TANDEM-MOTION PROGRAM

The "tandem-motion" program calculates time histories of specific energies and the corresponding adjoint variables for 2-D motion of two aircraft at a common altitude which is the "loft-ceiling" (highest altitude for vertical equilibrium in level flight) of the one identified as the pursuer (Refs. 7, 8, 9, 10). Energy modelling and a thrust-along-the-path assumption are employed as in the energy-turn program. Throttle is full forward ($\eta=1$) and wings level ($\mu=0$) for each aircraft.

Subscript 1 denotes evader and 2 pursuer. It should be noted that $\lambda_{E1} \geq 0$ and $\lambda_{E2} \leq 0$ for full-throttle flight in the differential-game formulations, i.e., the signs are normally _opposite._ This affords unusual opportunity for error in transition between the two-aircraft energy-turn program and the tandem-motion program, for in the former the signs of λ_{E1} and λ_{E2} are the _same_ for full throttle, both negative, this to permit use of the program for either aircraft singly in the same way as in the single-aircraft program (Ref. 6). The following adjoint equations account for the constraints $h_1 = h_2 - h_{2L}$ that specify both altitudes equal to the pursuer's loft-ceiling.

$$\dot{\lambda}_{E1} = -\lambda_{E1} \left\{ \frac{V_1}{W_1} \frac{\partial T_1}{\partial E_1} + \frac{T_1 g}{V_1 W_1} - \frac{q_1 S_1 g}{W_1} \left[\frac{1}{a} \frac{d C_{D_{o1}}}{d M_1} + \frac{3}{V_1} C_{D_{o1}} \right] \right.$$
$$\left. - \frac{W_1 g}{q_1 S_1 a} \left[\frac{d \frac{C_{D_2}}{C_L^2}}{d M_1} - \frac{\frac{C_{D_2}}{C_L^2}}{M_1} \right] \right\}$$

$$\dot{\lambda}_{E2} = -\lambda_{E2}\left\{\frac{V_2}{W_2}\frac{\partial T_2}{\partial E_2} - \frac{T_2 g}{V_2 W_2} - \frac{q_2 S_2 g}{W_2}\left[\frac{1}{a}\frac{dC_{D_{02}}}{dM_2} + \frac{3}{V_2}C_{D_{02}}\right]\right.$$

$$\left. - \frac{W_2 g}{q_2 S_2 a}\left[\frac{dC_{D_{C_{L_2}^2}}}{dM_2} - \frac{C_{D_{C_{L_2}^2}}}{M_2}\right]\right\}$$

$$- \lambda_{E2}\frac{dh_{2L}}{dE_2}\left\{\frac{V_2}{W_2}\frac{\partial T_2}{\partial h_2}\bigg|_{E_2} - \frac{g T_2}{V_2 W_2} + \frac{q_2 S_2 V_2}{W_2 a}\left(\frac{g}{V_2} + M_2\frac{da}{dh}\right)\frac{dC_{D_{o2}}}{dM_2}\right.$$

$$+ C_{D_{o2}}\left(\frac{3g q_2 S_2}{V_2 W_2} - \frac{S_2 V_2^3}{2 W_2}\frac{d\rho}{dh}\right)$$

$$\left. + \frac{2 W_2}{\rho_2 S_2 V_2}\left[\frac{dC_{D_{C_{L_2}^2}}}{dM_2}\left(\frac{g}{a V_2} + \frac{M_2}{a}\frac{da}{dh}\right) + C_{D_{C_{L_2}^2}}\left(\frac{1}{\rho}\frac{d\rho}{dh} - \frac{g}{V_2^2}\right)\right]\right\}$$

$$- \lambda_{E1}\frac{dh_{2L}}{dE_2}\left\{\frac{V_1}{W_1}\frac{\partial T_1}{\partial h_1}\bigg|_{E_1} - \frac{g T_2}{V_2 W_2} + \frac{q_1 S_1 V_1}{W_1 a}\left(\frac{g}{V_1} + M_1\frac{da}{dh}\right)\frac{dC_{D_{o1}}}{dM_1}\right.$$

$$+ C_{D_{o1}}\left(\frac{3g q_1 S_1}{V_1 W_1} - \frac{S_1 V_1^3}{2 W_1}\frac{d\rho}{dh}\right)$$

$$\left. + \frac{2 W_1}{\rho_1 S_1 V_1}\left[\frac{dC_{D_{C_{L_1}^2}}}{dM_1}\left(\frac{g}{a V_1} + \frac{M_1}{a}\frac{da}{dh}\right) + C_{D_{C_{L_2}^2}}\left(\frac{1}{\rho}\frac{d\rho}{dh} - \frac{g}{V_2^2}\right)\right]\right\}$$

INPUT SPECIFICATIONS, TANDEM-MOTION PROGRAM

The tandem-motion program has basically the same inputs as the two-vehicle energy-turn program.

A. Inputs for Preprocessor

NAMELIST/MINP/ATAB, HATB, CDOT, XMOT, CDCLT, XMCLT, RHT, HRT, TCLH, YMCL, TRXH, XMTRT, HTRT, NMA, NCDO, NCDCL, NRH, NCB, NXT, NHT, IDEN, IDG, LT, NEE, NE1, ETB

Notation Explanation

IDG
= 1 Generates power ceiling (h_6) and loft ceiling (h_7) tables versus energy.

= 0 Does not generate tables as they are already available.

NE1
Number of points to be splined in the power ceiling and loft-ceiling tables for Aircraft One.

NEE
Number of points for Aircraft Two, same tables as above.

ETB
Twenty point table of energies to be used when generating above tables.

All other terms are explained in the two-aircraft energy-turn section.

B. Main Inputs

1. Aircraft One — Evader

NAMELIST/MINPUT/GO, S, W, E, X, TMAX, DELT, NEQ, NPRN, ITB, INTB, CNCLC, XNB, ICB, XLE

ITB   = 1 Uses XLE input as initial λ_E for integration.

2.   Aircraft Two — Pursuer

NAMELIST/MINP2/S, W, E, CNCLC, XNB, ICB, XLE, EDOT

All other terms are explained in the two-vehicle energy-turn section.

Main inputs $MINPUT and $MINP2 must be read in at least twice for the first trajectory. The first time is needed for the preprocessing of the h_6 and h_7 tables.

C. Sample Input, Tandem-Motion Program

```
$MIMP
LT=2,
ETD=0.,5000.,10000.,15000.,20000.,25000.,30000.,35000.,40000.,45000.,
50000.,55000.,60000.,70000.,80000.,90000.,100000.,110000.,120000.,130000.,
NMA=20,
ATAB=1496.,1115.,1097.,1077.,1057.,1037.,1016.,994.7,968.1,968.1,968.1,
968.1,968.1,968.1,968.1,968.1,968.1,984.2,1004.,1056.43,
HATB=-1.E5,0.,5.E3,1.E4,1.5E4,2.E4,2.5E4,3.E4,3.503E4,4.E4,4.5E4,5.E4,
5.5E4,6.E4,7.E4,8.E4,8.202E4,9.E4,1.E5,2.E5,
NRH=20,
RHT=8957.E-6,2377.E-6,2048.E-6,1755.E-6,1496.E-6,1266.E-6,1065.E-6,
8893.E-7,7061.E-7,5851.E-7,4601.E-7,3618.E-7,2845.E-7,2238.E-7,
1384.E-7,8556.E-8,7764.E-8,5151.E-8,3131.E-8,94.E-8,
HRT=-1.E5,0.,5.E3,1.E4,1.5E4,2.E4,2.5E4,3.E4,3.509E4,4.E4,4.5E4,5.E4,
5.5E4,6.E4,7.E4,8.E4,8.202E4,9.E4,1.E5,2.E5,
NCB=14,
YMCL=0.,.1,.3,.5,.7,.9,1.1,1.3,1.5,1.7,1.3,2.1,2.3,2.6,0.,0.,0.,0.,0.,0.,
TCLH=.85,.85,.83,.81,.78,.68,.90,.75,.54,.45,.40,.35,.30,.3,
0.,0.,0.,0.,0.,0.,
NCDO=19,
CDOT=.0205,.0205,.0205,.0205,.0205,.0210,.0210,.0242,.0324,.0359,.0374,.0384,
.0385,.0386,.0387,.0397,.0403,.0403,.0403,0.,
XHDT=0.,.2,.65,.75,.80,.85,.90,.95,1.00,1.05,1.10,1.20,1.40,1.50,1.80,2.,
2.2,2.4,2.6,0.,
NCDCL=19,
CDCLT=.198,.198,.198,.201,.205,.211,.218,.228,.239,.252,.265,.297,.368,.453,
.544,.64,.744,.744,.744,0.,
XMCLT=0.,.2,.65,.75,.80,.85,.90,.95,1.0,1.05,1.10,1.20,1.40,1.60,1.80,2.,
2.2,2.4,2.6,0.,
NXT=14,NHT=10,
XMTRT=0.,.2,.4,.6,.8,1.,1.2,1.4,1.6,1.8,2.,2.2,2.4,2.6,0.,0.,0.,0.,0.,0.,
HTRT=-100000.,0.,10000.,20000.,30000.,40000.,50000.,60000.,70000.,
200000.,0.,0.,0.,0.,0.,0.,0.,0.,0.,0.,
TRXH(1,1)=120200.,120200.,117400.,108800.,119200.,102000.,33400.,2200.,5600.,
5600.,5600.,5600.,5600.,5600.,0.,0.,0.,0.,0.,0.,
TRXH(1,2)=32200.,32200.,33400.,34800.,39200.,42000.,41400.,40200.,39600.,
39600.,39600.,39600.,39600.,39600.,0.,0.,0.,0.,0.,0.,
TRXH(1,3)=23400.,23400.,25000.,27400.,31200.,36000.,42200.,44000.,43000.,
42000.,42000.,42000.,42000.,42000.,0.,0.,0.,0.,0.,0.,
TRXH(1,4)=16400.,16400.,17200.,19600.,23200.,27600.,32500.,38000.,42400.,
44000.,43000.,43000.,43000.,43000.,0.,0.,0.,0.,0.,0.,
TRXH(1,5)=11000.,11000.,11600.,13200.,16000.,19600.,24000.,28600.,33200.,
37200.,38500.,37800.,36800.,35800.,0.,0.,0.,0.,0.,0.,
TRXH(1,6)=6500.,6500.,7200.,8200.,10000.,12600.,15800.,19400.,23000.,
26400.,28400.,28600.,26800.,20400.,0.,0.,0.,0.,0.,0.,
TRXH(1,7)=4200.,4200.,4400.,5100.,5800.,7500.,9400.,11600.,14000.,16200.,
17600.,17800.,16400.,12300.,0.,0.,0.,0.,0.,0.,
TRXH(1,8)=2600.,2600.,2800.,3000.,3600.,4600.,5600.,7000.,8400.,9800.,
10600.,10800.,10200.,7600.,0.,0.,0.,0.,0.,0.,
TRXH(1,9)=2000.,2000.,2000.,2200.,2400.,2800.,3400.,4000.,4800.,5500.,
6200.,6400.,6000.,4600.,0.,0.,0.,0.,0.,0.,
TRXH(1,10)=20*0.,
IDEN=1,1,1,1,1,1,0,
$END
```

```
$MINP
LT=1,
NMA=20,NRH=20,
ATA3=1436.,1116.,1097.,1077.,1057.,1037.,1016.,994.7,968.1,963.1,368.1,
968.1,968.1,968.1,968.1,968.1,968.1,984.2,1004.,1056.43,
HAT3=-1.E5,0.,5.E3,1.E4,1.5E4,2.E4,2.5E4,3.E4,3.5093E4,4.E4,4.5E4,5.E4,
5.5E4,6.E4,7.E4,8.E4,8.2025E4,9.E4,1.E5,2.E5,
RHT=8957.E-6,2377.E-6,2043.E-6,1755.E-6,1496.E-6,1266.E-6,1063.E-6,
8493.E-7,7061.E-7,5851.E-7,4601.E-7,3618.E-7,2855.E-7,2238.E-7,
1384.E-7,9556.E-8,7764.E-8,5151.E-8,3131.E-8,94.E-8,
HRT=-1.E5,0.,5.E3,1.E4,1.5E4,2.E4,2.5E4,3.E4,3.5093E4,4.E4,4.5E4,5.E4,
5.5E4,6.E4,7.E4,8.E4,8.2025E4,9.E4,1.E5,2.E5,
NCB=16,
YMCL=0.,.2,.4,.6,.7,.8,.9,.95,1.,1.05,1.1,1.2,1.4,1.6,1.8,3.,4*0.,
TCL4=.85,.85,.86,.79,.76,.74,.84,1.04,1.2,1.27,1.23,1.13,.85,.65,.5,.5,
4*0.,
NCDO=16,
XMOT=0.,.2,.4,.6,.7,.8,.9,.95,1.,1.05,1.1,1.2,1.4,1.6,1.8,3.,4*0.,
CDOT=.02,.02,.0195,.0192,.0189,.0189,.0203,.027,.038,.0406,.0406,.0463,
.0414,.0413,.0413,.0413,4*0.,
NCDOL=16,
XMCLT=0.,.2,.4,.6,.7,.8,.9,.95,1.,1.05,1.1,1.2,1.4,1.6,1.8,3.,4*0.,
CDCLT=5.4,5.4,6.4,6.4,6.6,7.6,7.1,6.5,5.5,6.4,5.3,4.6,3.8,3.,2.5,2.5,4*0.,
NXT=10,NHT=9,
XHTRT=0.,.2,.4,.6,.8,1.,1.2,1.4,1.6,1.8,10*0.,
HTRT=-15000.,0.,15000.,25000.,36089.,40000.,45000.,50000.,175000.,11*0.,
TRXH(1,1)=9100.,9100.,9300.,10700.,11500.,12100.,13200.,14300.,15400.,
16500.,10*0.,
TRXH(1,2)=6600.,6600.,7200.,7900.,8700.,9500.,10300.,11100.,11900.,
12700.,10*0.,
TRXH(1,3)=4100.,4100.,4500.,5100.,5900.,6200.,7400.,7900.,8400.,8900.,
10*0.,
TRXH(1,4)=2500.,2500.,3000.,3500.,4100.,5000.,6100.,6900.,7300.,8700.,
10*0.,
TRXH(1,5)=1000.,1000.,1500.,2200.,2600.,3300.,4100.,4600.,5400.,6300.,
10*0.,
TRXH(1,6)=700.,700.,1200.,1700.,2200.,2800.,3400.,4000.,4600.,5200.,11*0.,
TRXH(1,7)=800.,800.,1100.,1400.,1700.,2100.,2700.,3200.,3700.,4200.,10*0.,
TRXH(1,8)=500.,500.,700.,1000.,1300.,1600.,2000.,2400.,2800.,3200.,10*0.,
TRXH(1,9)=20*0.,
IDEN=1,1,1,1,1,1,1,
$END
```

```
$MINP
IDG=1,NEE=12,LT=3,NE1=12,
NEE=18,NE1=18,
$END
$MINPUT
S=500.,W=36300.,INT3=1,CNCLC=1.5,XNB=6.7891,
W=9545.,XNB=7.33,ICB=1,S=170.,
GO=32.16,
            TMAX=600.,NPRN=13,DELT=-3.,NEQ=2,
TMAX=900.,
TMAX=30.,
$END
$MINP2
            ICB=1,S=530.,W=37523.,XNB=7.,
CNCLC=1.,
  $END
$MINPUT
E=45000.,
$END
$MINP2
E=46080.35,
$END
$MINPUT
INT3=0,
$END
$MINP
LT=0,
$END
```

OUTPUT, TANDEM-MOTION PROGRAM

Evader

T	E	PHE1	ALT	VEL
Q	MACH	MU	RHO	TR
D	L	CDO	CDB	CLB
CLH	CL	CDCL2	EDOT	HDIF
A	BET7	OME	H7	H6

If NEQ = 4, the following is printed.

LME1	LME2	CAPLH	LME1D	LME2D

Pursuer

T	E	PHE2	ALT	VEL
Q	MACH	PHEE	RHO	TR
D	L	CDO	CDB	CLB
CLH	CL	CDCL2	EDOT	
A	BET7	OMP	H7	H6

PHEE is analytical (closed-form) $(\partial h_7 / \partial E_2)$ printed as a check.

REFERENCES

1. Kelley, H. J.; "Aircraft Maneuver Optimization by Reduced-Order Approximation," in Vol. X of Advances in Control Systems, C. T. Leondes, Ed., Academic Press, New York, 1973.

2. Rutowski, E. S.; "Energy Approach to the General Aircraft Performance Problem," Journal of the Aeronautical Sciences, March 1954.

3. Boyd, J. R., Christie, T. P. and Drabant, R. E.; "Maximum Maneuver Concept," Air Force Armament Memorandum Report No. 71-2, Eglin Air Force Base, Florida, August 1971 (title unclassified).

4. Johnson, I. L. and Myers, G. E.; "One-Dimensional Minimization Using Search by Golden Section and Cubic Fit Methods," NASA Manned Spacecraft Center Internal Note 67-FM-172, November 13, 1967.

5. Mummolo, F. and Lefton, L.; "Cubic Splines and Cubic Spline Lattices for Digital Computation," Analytical Mechanics Associates, Inc. Report No. 72-28, July 1972; revision dated December 1974.

6. Lefton, L. and Krenkel, A. R.; "A User's Guide to the Supersonic Aircraft Energy-Turn Computer Program," Analytical Mechanics Associates, Inc. Report No. 72-12, August 1972; revision dated February 1975.

7. Lefton, L. and Kelley, H. J.; "A User's Guide to the Aircraft Energy-Turn Hodograph Program," Analytical Mechanics Associates, Inc. Report No. 75-7, March 1975.

8.   Kelley, H.J.; "Differential-Turning Optimality Criteria," Journal of Aircraft, January 1975.

9.   Kelley, H.J.; "Differential-Turning Tactics," Journal of Aircraft, to appear.

10.   Kelley, H.J. and Lefton, L.; "Computation of Differential-Turning Barrier Surfaces," Analytical Mechanics Associates, Inc. Report No. 75-27, September 1975.

A USER'S GUIDE TO THE

AIRCRAFT ENERGY-TURN HODOGRAPH PROGRAM

Leon Lefton
Henry J. Kelley

ABSTRACT

This manual is a guide to the use of the AIRCRAFT ENERGY-TURN HODO-
GRAPH PROGRAM which produces an extended energy-maneuverability description
of the capabilities of an aircraft whose characteristics have been input. The
various quantities computed are those needed in the energy-turn and differential-
tur analyses of the references. The program is in FORTRAN IV for use on a
CDC 6600 computer but with minor modifications can be run on any computer ac-
cer ng FORTRAN IV.

INTRODUCTION

The AIRCRAFT ENERGY-TURN HODOGRAPH PROGRAM is a computer
program for calculation of aircraft maneuvering performance in terms of the
following quantities as functions of specific energy level: maximum energy rate,
maximum instantaneous turn rate, maximum sustainable turn rate, power-ceiling,
loft-ceiling, energy rate at loft-ceiling, and loft-ceiling rate at loft-ceiling. A
choice of approximations for treatment of vertical thrust component is available
on input option.

The program is related to the SUPERSONIC AIRCRAFT ENERGY-TURN
COMPUTER PROGRAM of Refs. 1 and 2 and requires the same aircraft tabular
data represented via cubic-spline lattices (Ref. 3). The coding takes advantage
of the NAMELIST feature of FORTRAN IV, which permits 'stacking' of succes-
sive cases to be computed with minimal input. The program may be used in
conjunction with the two programs of Ref. 7, as described in Ref. 8, to generate
families of differential-turn trajectories and their barrier surfaces.

1

ANALYTICAL DESCRIPTION

Turning duels between two dissimilar aircraft are studied in Refs. 4, 5, and 6 with the use of energy modelling approximation and a differential game formulation. Computation of various energy-rate and turn-rate quantities are needed for comparisons which represent steps in the numerical solution of the differential-turning game, and which are in themselves of more than qualitative interest for comparison of configurations.

Power-Ceiling at a specified energy level is defined as the highest altitude permitting horizontal-force equilibrium in level flight. Designated h_6, it is determined implicitly by

$$T\left(1 - \frac{\alpha^2}{2}\right) - D = 0 \qquad (1a)$$

with α from

$$q \, S \, C_{L_\alpha} \, \alpha + T\alpha = W \qquad (2a)$$

The computation is performed with Specific Energy, $E = h + V^2/2g$ held constant. An alternate thrust-along-the-path option is available with use of

$$T - D = 0 \qquad (1b)$$

$$q \, S \, C_{L_\alpha} \, \alpha = W \qquad (2b)$$

Either eq. (1a) or (1b) is solved computationally by Newton-Raphson iteration beginning with a first guess determined by a rough scan over the altitude range. A quadratic C_D versus C_L model is employed, with no upper bound imposed upon C_L.

<u>Loft-Ceiling</u>, h_7, is defined as the highest altitude permitting vertical equilibrium. It is determined as the root of

$$q S \hat{C}_L(M) + T \sin \alpha^* = W \tag{3}$$

where $\hat{C}_L(M)$ is $C_{L_{max}}$, a function of Mach number. Stall angle-of-attack, α^*, may be input as zero for thrust-along-the-path modelling; this choice also triggers the use of (1a) and (2a) in preference to (1b) and (2b).

<u>Sustainable Turn Rate</u> is computed in small-α approximation as

$$\omega_p = \frac{g \sin \mu}{VW} (L + T\alpha) \tag{4a}$$

A candidate α is computed from the horizontal-force-equilibrium eq. (1b); it is employed if the corresponding lift coefficient $C_L = C_{L_\alpha} \alpha \leq \hat{C}_L$; otherwise $\hat{C}_L$ and corresponding $\hat{\alpha}$ are used in (4a). Computations are performed at fixed E and h. The maximum sustainable turn rate for each E is picked out by a scan over the altitude range bounded below by terrain limit, h_1, dynamic pressure limit, h_2, or Mach number limit, h_3, and bounded above by h_6. The altitude bounds h_2 and h_3 are determined by iterative solution of the defining equations $\beta_2 = 0$ and $\beta_3 = 0$ as in Refs. 1 and 2; in fact, the coding employed is identical. The approximation to the maximum sustainable turn rate found by the scan over a coarse mesh is further refined by the use of golden-section one-dimensional search starting at the altitude mesh-point chosen by the scan.

An alternative estimate of sustainable turn rate employing a thrust-along-the-path model is triggered by input of $\alpha^* = 0$. (The estimate of the preceding paragraph is automatic for $\alpha^* \neq 0$, as is the power-ceiling estimate of eqs. (1a) and (2a).) It is important to input $\alpha^* = 0$ when compatibility with the program of Refs. 1 and 2 is needed. The thrust-along-the-path model uses $\cos \alpha = 1$, $\sin \alpha = 0$, obtains a C_L candidate as

3

$$C_L = \sqrt{\frac{1}{C_{D_{C_L^2}}}\left(\frac{T}{q\,s} - C_{D_o}\right)} \qquad (5)$$

and employs it if $< \hat{C}_L$, otherwise $\hat{C}_L$ in

$$\omega_p = \frac{g \sin \mu \, q \, S \, \hat{C}_L}{V\,W} \qquad (4b)$$

Maximum Instantaneous Turn Rate is computed as that for $C_L = \hat{C}_L$ at the corner-velocity altitude, h_{45}, if $h_{45} \geq 0$ for the chosen energy level, otherwise at $h = 0$. The corner-velocity altitude is determined by iteration on $\beta_4 = 0$ and $\beta_5 = 0$ (C_L limit and normal-load-factor limit) just as in the program of Refs. 1 and 2.

$$\omega_L = \frac{g}{V} \sqrt{\left(\frac{q\,S\,\hat{C}_L + T \sin \alpha^*}{W}\right)^2 - 1} \qquad (6)$$

Energy Rate is computed in small-α approximation as

$$\dot{E} = V\left[T\left(1 - \frac{\alpha^2}{2}\right) - D\right] \qquad (7a)$$

with α determined from eq. (2b) at each specified energy-altitude point. This approximation is used when $\alpha^* \neq 0$ is input whereas, for $\alpha^* = 0$, a thrust-along-the-path model is used for which the corresponding equations are

$$\dot{E} = V[T - D] \qquad (7b)$$

and α determined by

$$q\,S\,C_{L_\alpha}\,\alpha = W \qquad (2c)$$

Standard print-out for both options consists of the maximum energy-rate value at each specific energy level, determined by a scan plus search between bounds identical to that for maximum sustainable turn rate, and the energy rate at h_7, the loft-ceiling. Also printed is time rate of change of loft-ceiling altitude.

TURN RATE COMPARISONS

When the characteristics of two aircraft are input, computational comparison of sustainable turn-rates is carried out. One such computation determines the curve in energy space separating regions of sustainable-turn-rate superiority of each craft over the other; the other compares sustainable turn rates at matched loft-ceilings (Refs. 4 and 5). Prior to these computations, cubic spline fits are made of maximum sustainable turn rate versus specific energy and loft-ceiling versus specific energy for both aircraft. The computations then proceed iteratively for several input values of sustainable turn rate, yielding as many as four pairs of energies for each. It should be noted that the equal-sustainable-turn-rate curves in energy space enter the determination of the number and sequence of subarcs of trajectories and affect the barrier surface structure.

A similar computation of pairs of energies for equal instantaneous turn rates is available on option.

TANDEM/LOFT MOTION APPROXIMATION

A rough estimate of the tandem/loft motion starting at the matched-loft-ceiling curve and proceeding for a single step backwards in time is provided by Euler extrapolation. If $(\dot{h}_{L2} - \dot{h}_{L1}) \geq 0$ at loft-ceiling match, tandem/loft motion is a candidate option for the pursuer and, accordingly, the computation is performed; otherwise it is by-passed. If the second derivative of the rate difference $(\ddot{h}_{L2} - \ddot{h}_{L1})$ is positive, the time step

$$\Delta t = - \frac{(\dot{h}_{L2} - \dot{h}_{L1})}{(\ddot{h}_{L2} - \ddot{h}_{L1})} \tag{8}$$

5

is calculated and employed so long as it does not exceed in magnitude an input value $\overline{\Delta t} < 0$, chosen as perhaps -20 sec. or -30 sec. If the second derivative is not positive or if Δt given by (8) exceeds $\overline{\Delta t}$ in magnitude, $\overline{\Delta t}$ is used. The pair of extrapolated energies and the Δt used are calculated and printed for various initial points along the matched-loft-ceiling curve.

CHATTERING SINGULAR ARC

The locus of a singular solution in energy space (Ref. 6) is determined upon input option by iteration on $\Delta = 0$, Δ being a determinant having pursuer and evader energies as arguments.

$$\Delta = \left(f_{2L} - f_2^* \right) \left(f_1^* \frac{\partial f_{12L}}{\partial E_1} - f_{12L} \frac{\partial f_1^*}{\partial E_1} + f_2^* \frac{\partial f_{12L}}{\partial E_2} \right)$$

$$- \left(f_{12L} - f_1^* \right) \left(f_2^* \frac{\partial f_{2L}}{\partial E_2} - f_{2L} \frac{\partial f_2^*}{\partial E_2} \right) = 0$$

where

$$f_1^* \equiv \left[-\frac{V_1(T_1 - D_1)}{W_1} \right]_{h_1^*} \quad , \quad f_2^* \equiv \left[\frac{V_2(T_2 - D_2)}{W_2} \right]_{h_2^*}$$

$$f_{2L} \equiv \left[\frac{V_2(T_2 - D_2)}{W_2} \right]_{h_{2L}} \quad , \quad f_{12L} \equiv \left[\frac{V_1(T_1 - D_1)}{W_1} \right]_{h_{2L}}$$

$$\frac{\partial f_1^*}{\partial E_1} = \frac{\partial}{\partial E_1} \left[\frac{V_1(T_1 - D_1)}{W_1} \right]_{h_1^*} + \frac{\partial}{\partial h_1} \left[\frac{V_1(T_1 - D_1)}{W_1} \right]_{h_1^*} \frac{dh_1^*}{dE_1}$$

$$\frac{\partial f_2^*}{\partial E_2} = \frac{\partial}{\partial E_2} \left[\frac{V_2(T_2 - D_2)}{W_2} \right]_{h_2^*} + \frac{\partial}{\partial h_2} \left[\frac{V_2(T_2 - D_2)}{W_2} \right]_{h_2^*} \frac{dh_2^*}{dE_2}$$

$$\frac{\partial f_{12L}}{\partial E_1} = \frac{\partial}{\partial E_1} \left[\frac{V_1(T_1 - D_1)}{W_1} \right]_{h_{2L}}$$

$$\frac{\partial f_{12L}}{\partial E_2} = \frac{\partial}{\partial h_1} \left[\frac{V_1(T_1 - D_1)}{W_1} \right]_{h_{2L}} \frac{dh_{2L}}{dE_2}$$

$$\frac{\partial f_{2L}}{\partial E_2} = \frac{\partial}{\partial E_2}\left[\frac{V_2(T_2 - D_2)}{W_2}\right]_{h_{2L}} + \frac{\partial}{\partial h_2}\left[\frac{V_2(T_2 - D_2)}{W_2}\right]_{h_{2L}} \frac{\partial h_{2L}}{\partial E_2}$$

In these expressions, h_i^* is the altitude for maximum energy rate f_i^*, and h_{2L} is the pursuer's loft-ceiling altitude.

The locus of points for which Δ vanishes subject to the evader's loft-ceiling exceeding the pursuer's is of interest. To determine this approximately, a scan is carried out of Δ versus evader energy at fixed pursuer energy, using the loft-ceiling match energy previously determined as a lower bound. A more precise determination is then performed by minimization of Δ^2 via golden-section search. This is done for several input values of pursuer energy.

Since the computer program employs cubic-spline fits of $h^*(E)$ and first derivatives of these spline representations, care must be taken when $h^*(E)$ for either or both aircraft exhibits a jump discontinuity to carry out the chattering arc computations sectionally, i. e. , not requiring the spline to approximate the discontinuous function, so as to avoid undue numerical error.

INPUT SPECIFICATIONS

A   Input Tables

NAMELIST/MINP/ATAB, HATB, CDOT, XMOT, CDCLT, XMCLT, RHT,

       HRT, TCLH, YMCL, TRXH, XMTRT, HTRT, NMA, NCDO,

       NCDCL, NRH, NCB, NXT, NHT, IDEN, LT, EMIN, EMID,

       EMAX, DEMID, DEMAX, ETA, IDG0, IDG1, IDG2, IDSUS,

       EVL, ISEP, DLTI, IMXI

IDEN is dimensioned 6 and each slot is associated with a table IP. The
tables are as follows:

ID	TABLE	DIMENSION	NUMBER OF POINTS	DESCRIPTION
1	ATAB	20	NMA	a (speed of sound)
1	HATB	20	NMA	h (altitude)
2	CDOT	20	NCDO	C_{D_o}
2	XMOT	20	NCDO	Mach Number
3	CDCLT	20	NCDCL	$C_{D_{C_L^2}}$
3	XMCLT	20	NCDCL	Mach Number
4	RHT	20	NRH	ρ (density)
4	HRT	20	NRH	h (altitude)
5	TCLH	20	NCB	$\hat{C}_L$
5	YMCL	20	NCB	Mach Number
6	TRXH	20, 20	NXT, NHT	TR (thrust)
6	XMTRT	20	NXT	Mach Number
6	HTRT	20	NHT	h (altitude)
	EVL	100		Energy to be processed

Other notation explanation:

LT	= 0 indicates end of run (termination trigger)
	= 1 indicates evader processed
	= 2 indicates pursuer processed
EMIN	minimum E
EMID	internal cutoff E
EMAX	maximum E
DEMID	ΔE from EMIN to EMID; if DEMID = 0 , program expects EVL table
DEMAX	ΔE from EMID to EMAX
ETA	constant multiplier of thrust tables
IDG0	= 1 processes evader when two-aircraft study is desired
	= 2 pursuer processed
	= 3 one aircraft study to be followed by study of another aircraft
	=4 one aircraft study to be followed with another study using the same aircraft
IDG1	=1 normal print
	= 2 skips table prints other than matchings
IDG2	= 1 no chattering
	= 2 includes chattering
IDSUS	number of points in grid of matching maximum sustainable turn rates
ISEP	= 0 no approximate tandem loft motion
	$\neq 0$ calculates and prints approximate tandem-loft motion
DLTI	limit on Δ in tandem-loft motion; must be positive
IMXI	number of points in grid of maximum instantaneous matchings

B   Other Input

NAMELIST/MINPUT/GO, S, W, CNCLC, XNB, QBAR, XMBAR, EB3,
HT, ICB, ALPN, ALPD

Notation Explanation

GO	gravitational constant (32.16)
S	wing planform reference area
W	weight of aircraft
CNCLC	speed brake factor, where $C_{D_B} = CNCLC * C_{D_o}$
XNB	N (maximum structural load factor)
QBAR	Q boundary for β_2 calculation
XMBAR	Mach boundary for β_3 calculation
EB3	If $E < EB3$, by-pass β_3 calculation
HT	maximum altitude allowed
ICB	$= 0$, $\hat{C}_L = 1$
	$= 1$, $\hat{C}_L = TCLH \text{ (MACH)}$
ALPN	numerator for α^*
ALPD	denominator for α^*

OUTPUT

Sample output follows.

.

10

MONOGRAPH RATE DATA

PROGRAMMED BY ANALYTICAL MECHANICS ASSOCIATES INC.

ALPHA* = 0.0   PURSUER= F4

POWER CEILING	POWER-CEILING TURN RATE	LOFT CEILING	PAR-LFT-CEIL TO ENERGY	ALTITUDE LOWER BOUND	LOWER AND TURN RATE	MAX SUSTNBLE TURN RATE ALT	MAX SUSTNBLE TURN RATE	SPECIFIC ENERGY
4.712533E+03	0.	3.751652E+03	9.537562E-01	0.	2.414365E-01	0.	2.414565E-01	5.000000E+03
9.605431E+03	0.	8.559709E+03	9.564531E-01	0.	2.559428E-01	0.	2.559425E-01	1.000000E+04
1.445434E+04	0.	1.331341E+04	9.482797E-01	0.	2.434790E-01	0.	2.434790E-01	1.500000E+04
1.923853E+04	0.	1.803031E+04	9.371345E-01	0.	1.631225E-01	4.462959E+03	2.172539E-01	2.000000E+04
2.332980E+04	0.	2.267423E+04	9.244365E-01	0.	6.999627E-02	9.604168E+03	1.308726E-01	2.500000E+04
2.848611E+04	0.	2.724903E+04	9.073731E-01	5.989759E+02	-1.000000E+03	1.485400E+04	1.545142E-01	3.000000E+04
3.286826E+04	0.	3.175204E+04	8.953514E-01	3.528930E+03	-1.000000E+03	2.022841E+04	1.384941E-01	3.500000E+04
3.697353E+04	0.	3.614267E+04	8.544819E-01	6.036023E+03	-1.000000E+03	2.564243E+04	1.137135E-01	4.000000E+04
4.071765E+04	0.	4.029459E+04	8.126500E-01	8.432145E+03	-1.000000E+03	1.751015E+04	9.856445E-02	4.500000E+04
4.417703E+04	0.	4.427331E+04	7.734327E-01	1.072934E+04	-1.000000E+03	2.026893E+04	8.753915E-02	5.000000E+04
4.725571E+04	0.	4.735628E+04	6.764134E-01	1.290397E+04	-1.000000E+03	2.283783E+04	7.943782E-02	5.500000E+04
4.996541E+04	0.	5.194707E+04	5.312121E-01	1.499454E+04	-1.000000E+03	2.472776E+04	7.221604E-02	6.000000E+04
5.243478E+04	0.	5.750526E+04	7.762103E-01	1.833439E+04	0.	2.745930E+04	5.432275E-02	7.000000E+04
5.409070E+04	1.224475E-03	6.484932E+04	8.258081E-01	2.234072E+04	-1.000000E+03	3.206688E+04	4.748956E-02	8.000000E+04
5.553177E+04	9.466416E-03	7.129955E+04	4.525563E-01	2.552427E+04	-1.000000E+03	3.772413E+04	3.582927E-02	9.000000E+04
5.613480E+04	0.	7.279608E+04	1.666286E+00	2.841490E+04	-1.000000E+03	4.152250E+04	2.397594E-02	1.000000E+05
5.328999E+04	0.	7.253192E+04	-1.344702E+01	3.112899E+04	-1.000000E+03	4.574382E+04	3.481281E-03	1.100000E+05

11

ALT-FOR-MAX INST-TRN-RT	MAX-INST. TURN-RATE	ALT-FOR-MAX ENERGY-RATE	MAXIMUM ENERGY-RATE	MAX-LOFT CEIL-RATE	ENERGY-RATE AT-LOFT-CEIL	LOFT-CEIL-RT AT-LOFT-CEIL	SPECIFIC-ENER
0.	2.414365E-01	0.	4.291420E+02	4.135542E+02	1.651851E+02	1.559970E+02	5.000000E+03
1.497610E+03	3.012353E-01	0.	6.037494E+02	5.777046E+02	1.453541E+02	1.364058E+02	1.000000E+04
5.075832E+03	2.744335E-01	0.	7.204452E+02	6.835257E+02	1.253034E+02	1.163106E+02	1.500000E+04
8.142524E+03	2.551335E-01	3.671453E+03	6.867355E+02	6.435276E+02	1.055747E+02	9.607936E+01	2.000000E+04
1.137912E+04	2.330461E-01	9.045141E+03	6.251250E+02	5.773259E+02	8.613120E+01	7.732471E+01	2.500000E+04
1.515597E+04	2.230278E-01	1.433495E+04	5.437387E+02	4.989733E+02	6.861823E+01	6.074908E+01	3.000000E+04
1.918130E+04	2.203911E-01	1.983709E+04	4.631307E+02	4.146757E+02	5.072263E+01	4.477850E+01	3.500000E+04
2.323691E+04	2.145787E-01	1.454443E+04	4.341044E+02	3.743523E+02	3.163225E+01	2.722294E+01	4.000000E+04
2.711614E+04	2.077462E-01	1.722098E+04	4.124045E+02	3.352100E+02	1.365969E+01	1.111135E+01	4.500000E+04
3.051701E+04	1.990379E-01	2.013140E+04	3.975449E+02	3.074897E+02	-2.649010E+00	-1.942485E+00	5.000000E+04
3.252031E+04	1.852970E-01	2.303193E+04	3.934105E+02	2.703299E+02	-1.653594E+01	-9.231872E+00	5.500000E+04
3.224047E+04	1.658671E-01	2.520581E+04	4.012320E+02	2.131676E+02	-2.303040E+01	-9.137468E+00	6.000000E+04
3.197072E+04	1.424638E-01	2.851663E+04	3.892441E+02	3.021355E+02	-5.436917E+01	-5.445805E+01	7.000000E+04
3.187977E+04	1.293653E-01	3.360489E+04	3.575341E+02	2.952717E+02	-1.412779E+02	-1.516689E+02	8.000000E+04
3.550724E+04	1.171223E-01	3.903003E+04	2.935354E+02	1.328997E+02	-2.316854E+02	-1.139454E+02	9.000000E+04
3.666854E+04	1.103361E-01	4.236317E+04	1.819652E+02	3.031922E+02	-2.772366E+02	2.173291E+01	1.000000E+05
3.701131E+04	1.028338E-01	4.610136E+04	3.961963E+01	-5.325536E+02	-2.983134E+02	-3.270466E+01	1.100000E+05

HODOGRAPH RATE DATA

PROGRAMMED BY ANALYTICAL MECHANICS ASSOCIATES INC.

ALPHA*= 0.0   EVADER= HYPO

POWER CEILING	POWER-CEILING TURN RATE	LOFT CEILING	PAR-EFT-CEIL TO ENERGY	ALTITUDE LOWER BOUND	LOWER BND TURN RATE	MAX SUSTNBLE TURN RATE ALT	MAX SUSTNBLE TURN RATE	SPECIFIC ENERGY
4.142388E+03	0.	3.441405E+03	9.643721E-01	0.	1.423653E-01	0.	1.429653E-01	5.000000E+03
8.858779E+03	0.	8.772195E+03	9.632223E-01	0.	1.507697E-01	0.	1.507697E-01	1.000000F+04
1.346402F+04	2.225964E-06	1.357125E+04	9.580941E-01	0.	1.553972E-01	0.	1.553972E-01	1.500000E+04
1.792196F+04	1.420511E-06	1.432964F+04	9.457343E-01	2.901042E+03	1.427962E-01	2.901042F+03	1.427962E-01	2.000000E+04
2.220084E+04	7.568856E-07	2.303762C+04	9.362774F-01	6.136771F+03	1.281270E-01	6.136771E+03	1.281270E-01	2.500000E+04
2.628560F+04	0.	2.763407E+04	9.224772E-01	9.234716E+03	1.143428E-01	9.238706E+03	1.143428E-01	3.000000E+04
3.019593E+04	0.	3.227113E+04	9.106011E-01	1.220589F+04	1.026868E-01	1.220589E+04	1.026868E-01	3.500000E+04
3.392871E+04	0.	3.643546E+04	8.690720E-01	1.503187E+04	9.393312E-02	1.503187E+04	9.393312E-02	4.000000E+04
3.730016E+04	0.	4.098430E+04	8.369045E-01	1.771326E+04	8.784476E-02	1.771326E+04	8.784476E-02	4.500000E+04
4.022043E+04	0.	4.510475E+04	8.105756E-01	2.026271E+04	8.293742E-02	2.026271E+04	8.299742E-02	5.000000E+04
4.276032E+04	0.	4.998026E+04	7.740477E-01	2.268923E+04	7.833548E-02	2.268923E+04	7.33354RE-02	5.500000E+04
4.493859E+04	0.	5.284935E+04	7.453338E-01	2.498394E+04	7.420893E-02	2.498394E+04	7.420893E-02	6.000000E+04
4.866761F+04	0.	5.939757E+04	6.755525E-01	2.921049E+04	7.001840E-02	2.921049E+04	7.001840E-02	7.000000E+04
5.246070E+04	0.	6.539905E+04	6.046175E-01	3.310893E+04	6.638387E-02	3.310898E+04	6.638387E-02	8.000000E+04
5.600832E+04	0.	7.210032E+04	5.367789E-01	3.640536E+04	6.127722E-02	3.640536E+04	6.127722E-02	9.000000E+04

ALT-FOR-MAX DIST-TRN-RT	MAX-DIST. TURN-RAT.	ALT-FOR-MAX ENERGY-RATE	MAXIMUM ENERGY-RATE	MAX-LOFT CEIL-RATE	ENERGY-RATE AT-LOFT-CEIL	LOFT-CEIL-RT AT-LOFT-CEIL	SPECIFIC-ENER
0.	2.456519E-01	0.	2.910041E+02	2.820159E+02	2.784431E+01	2.698037E+01	5.000000E+03
3.011655E+03	3.221117E-01	0.	4.545464E+02	4.379277E+02	9.861132E+00	9.498468E+00	1.000000E+04
7.988227E+03	3.072999E-01	0.	5.925573E+02	5.664779E+02	-1.004519E+01	-9.603243E+00	1.500000E+04
1.104902E+04	2.846144E-01	2.901842E+03	5.833751E+02	5.528313E+02	-3.131048E+01	-2.964473E+01	2.000000E+04
1.487975E+04	2.676531E-01	6.156771E+03	5.464120E+02	5.116149E+02	-5.293196E+01	-4.958711E+01	2.500000E+04
1.855311E+04	2.517398E-01	9.234706E+03	5.042377E+02	4.651462E+02	-7.383943E+01	-6.816132E+01	3.000000E+04
2.210193E+04	2.373955E-01	1.229543E+04	4.636463E+02	4.277078E+02	-3.505742E+01	-9.655040E+01	3.500000E+04
2.548086E+04	2.214713E-01	1.503147E+04	4.528377E+02	3.935320E+02	-1.203750E+02	-1.046145E+02	4.000000E+04
2.859213E+04	2.175971E-01	1.771326E+04	4.555702E+02	3.813575E+02	-1.530904E+02	-1.281221E+02	4.500000E+04
3.178977E+04	1.905421E-01	2.026271E+04	4.670190E+02	3.785451E+02	-1.867162E+02	-1.513476E+02	5.000000E+04
3.469771E+04	1.813417E-01	2.261923E+04	4.756305E+02	3.708177E+02	-2.162723E+02	-1.682702E+02	5.500000E+04
3.727244E+04	1.716141E-01	2.436334E+04	4.931312E+02	3.546852E+02	-2.431522E+02	-1.812295E+02	6.000000E+04
4.173510E+04	1.611553E-01	2.921743E+04	5.549757E+02	3.816100E+02	-2.965769E+02	-2.003829E+02	7.000000E+04
4.575313E+04	1.455363E-01	3.319898E+04	6.478304E+02	3.917020E+02	-3.565206E+02	-2.155586E+02	8.000000E+04
4.332785E+04	1.351492E-01	3.548536E+04	6.931521E+02	3.752955E+02	-4.243676E+02	-2.280600E+02	9.000000E+04

DUAL HODOGRAPH DATA
LOFT-CEILING-MATCHED RATES

EVAPER-E	PUR-TN MATCHED	MAX-INST-TRN RATE-EV	MAX-INST-TRN RATE-PUR	MARGIN	LF-CEIL-RT-AT LFT-CEIL-EV	LF-CEIL-RT-AT LFT-CEIL-PUR	MARGIN
5.000000E+03	5.137009E+03	2.956019E-01	2.404405E-01	-4.922148E-02	2.698037E+01	1.553106E+02	1.283303E+02
1.000000E+04	1.022229E+04	3.221197E-01	3.003505E-01	-2.174595E-02	9.493468E+00	1.355119E+02	1.260134E+02
1.500000E+04	1.526713E+04	3.027299E-01	2.776117E-01	-2.512820E-02	-9.603243E+00	1.152302E+02	1.248335E+02
2.000000E+04	2.032341E+04	2.846144E-01	2.537545E-01	-3.085602E-02	-2.964473E+01	9.479249E+01	1.244372E+02
2.500000E+04	2.539441E+04	2.676481E-01	2.370533E-01	-3.061413E-02	-4.958711E+01	7.595786E+01	1.255458E+02
3.000000E+04	3.048370E+04	2.517898E-01	2.272548E-01	-2.452161E-02	-6.816132E+01	5.921879E+01	1.273801E+02
3.500000E+04	3.553164E+04	2.370535E-01	2.201379E-01	-1.696168E-02	-3.653940E+01	4.280563E+01	1.293650E+02
4.000000E+04	4.069650E+04	2.234713E-01	2.156487E-01	-9.782544E-03	-1.046145E+02	2.477901E+01	1.293935E+02
4.500000E+04	4.585801E+04	2.108547E-01	2.064485E-01	-4.411181E-03	-1.281221E+02	8.681728E+00	1.368038E+02
5.000000E+04	5.108016E+04	1.995421E-01	1.966299E-01	-2.913533E-03	-1.513475E+02	-4.319072E+00	1.470285E+02
5.500000E+04	5.674493E+04	1.869917E-01	1.749278E-01	-1.005465E-02	-1.682702E+02	-8.958885E+00	1.593113E+02
6.000000E+04	6.299316E+04	1.786141E-01	1.573921E-01	-2.122200E-02	-1.812295E+02	-1.397098E+01	1.672585E+02
7.000000E+04	7.350566E+04	1.501953E-01	1.373242E-01	-2.284111E-02	-2.003829E+02	-8.974326E+01	1.106397E+02
8.000000E+04	8.205597E+04	1.455063E-01	1.270345E-01	-1.841253E-02	-2.155586E+02	-1.646790E+02	5.087958E+01
9.000000E+04	9.249777E+04	1.335192E-01	1.168467E-01	-1.669255E-02	-2.280600E+02	-6.157353E+01	1.664363E+02

DUAL MONOGRAPH DATA
LOFT-CEILING-MATCHED RATES

EVAPTR-E	PUR-EN MATCHED	LOFT-CEIL	SUS-TRN-RT-EV	SUS-TN-RT-PUR	MARGIN	MAX-LOFT-CEIL-RT-EV	MAX-LOFT-CEIL-RT-PUR	MARGIN
5.000000E+03	5.147009E+03	3.341405E+03	1.423957E-01	2.422121E-01	3.924682E-02	2.820369E+02	4.199317E+02	1.374948E+02
1.000000E+04	1.022229E+04	8.772735E+03	1.517547E-01	2.559352E-01	1.052265E-01	4.379277E+02	5.344674E+02	1.465397E+02
1.500000E+04	1.525713E+04	1.357125E+04	1.553172E-01	2.422495E-01	8.085124E-02	5.664779E+02	6.847434E+02	1.182655E+02
2.000000E+04	2.032341E+04	1.832764E+04	1.427165E-01	2.154934E-01	7.270322E-02	5.528313E+02	6.390977E+02	8.626636E+01
2.500000E+04	2.539441E+04	2.303732E+04	1.281273E-01	1.889011E-01	6.057407E-02	5.116689E+02	5.724431E+02	6.077423E+01
3.000000E+04	3.048070E+04	2.768507E+04	1.143423E-01	1.620143E-01	4.767147E-02	4.651662E+02	4.902162E+02	2.505002E+01
3.500000E+04	3.558164E+04	3.227113E+04	1.026369E-01	1.354003E-01	3.271347E-02	4.277078E+02	4.079400E+02	-1.976776E+01
4.000000E+04	4.069690E+04	3.673566E+04	9.393112E-02	1.110256E-01	1.704249E-02	3.935920E+02	3.692249E+02	-2.436714E+01
4.500000E+04	4.585361E+04	4.093706E+04	8.784767E-02	9.650537E-02	8.661205E-03	3.813525E+02	3.295713E+02	-5.178054E+01
5.000000E+04	5.104016E+04	4.510475E+04	8.297742E-02	8.559411E-02	2.586687E-03	3.785461E+02	3.017811E+02	-7.676505E+01
5.500000E+04	5.674493E+04	4.908026E+04	7.833549E-02	7.687324E-02	-1.462241E-03	3.708177E+02	2.477642E+02	-1.230535E+02
6.000000E+04	6.299316E+04	5.288935E+04	7.420899E-02	6.814751E-02	-6.061318E-03	3.646032E+02	2.172179E+02	-1.473854E+02
7.000000E+04	7.350566E+04	5.993757E+04	7.001440E-02	5.512314E-02	-1.489526E-02	3.816800E+02	3.328602E+02	-4.881984E+01
8.000000E+04	8.205697E+04	6.639405E+04	6.538587E-02	4.507392E-02	-2.131086E-02	3.917020E+02	2.495994E+02	-1.421026E+02
9.000000E+04	9.243777E+04	7.210432E+04	6.127722E-02	3.293747E-02	-2.823975E-02	3.752955E+02	1.868586E+02	-1.884369E+02

REFERENCES

1. Lefton, L. and Krenkel,A. R.;"A User's Guide to the Supersonic Aircraft Energy Turns Computer Program," Analytical Mechanics Associates, Inc. Report No. 72-12, August 1972.

2. Kelley, H. J.; "Aircraft Maneuver Optimization by Reduced-Order Approximation," in Vol. X of Controls and Dynamic Systems: Advances in Theory and Applications, C. T. Leondes, ed., Academic Press, New York, 1973.

3. Mummolo, F. and Lefton, L.; "Cubic Splines and Cubic Spline Lattices for Digital Computation," Analytical Mechanics Associates, Inc. Report No. 72-28, July 1972.

4. Kelley, H. J. and Lefton, L.; "Differential Turns," AIAA Atmospheric Flight Mechanics Specialists Conference, Palo Alto, California, September 11-13, 1972; also AIAA Journal, Vol. 11, No. 6, June 1973, pp. 858-861.

5. Kelley, H. J.; "Differential Turning Optimality Criteria," AIAA 12th Aerospace Sciences Meeting, Washington, D. C., January 30-February 1, 1974; Journal of Aircraft, Vol. 12, No. 1, January 1975.

6. Kelley, H. J.; "Differential Turning Tactics," AIAA Mechanics and Control of Flight Conference, Anaheim, California, August 5-9, 1974; to appear in Journal of Aircraft.

7. Lefton, L., Krenkel, A. R. and Kelley, H. J.; "A User's Guide to the Aircraft Energy-Turn and Tandem-Motion Computer Programs," Analytical Mechanics Associates, Inc. Report No. 75-26, June 1975, revised January 1976.

8. Kelley, H. J. and Lefton, L.; "Calculation of Differential-Turning Barrier Surfaces," Analytical Mechanics Associates, Inc. Report No. 75-27, September 1975.